interpretation of basal-like immunopanels are necessary before clinical application. Regular participation of laboratories in external quality assurance and proficiency testing programs will facilitate implementation.

Techniques

2116 In-Situ Redox Profiling of Diffuse Large B-Cell Lymphoma

SW Aesif, L Taylor, I Kuipers, L DePalma. The George Washington University, Washington, DC; National Institutes of Health, Bethesda, MD.

Background: Methods for the histochemical detection of tissue thiols have been described in the literature. These methods are incompatible with routine histology given their complex chemistries and need for specialized microscopy. Further, there is scant data evaluating the in-situ distribution and concentration of free protein thiols (i.e. -SH or sulfhydrals) and reducible protein thiols (i.e. disulfides, mixed disulfides, nitrosothiols, and sulfenic acids) in human tissues.

Design: Contemporary literature has recently likened post-translational protein thiol oxidation to *O*-phosphorylation, with regard to its role in cell signal transduction, enzyme function, protein structure, and disease pathogenesis. We therefore sought to explore the distribution and concentration of free and reducible protein thiols, by developing a staining technique using modern histochemical reagents that allow for the visualization of tissue protein thiols in-situ, under bright field microscopy.

Results: The thiol staining technique was developed and validated using routinely available control tissue. The thiol staining technique was then used to assess benign tonsillectomy specimens, benign surgical lymph node specimens, and excisional lymph node biopsy specimens diagnosed as involved by diffuse large B-cell lymphoma (DLBCL). In both the tonsils and lymph nodes, we observed a robust presence of free protein thiols. Germinal center cells contained appreciably more free protein thiols than the surrounding small lymphocytes. When we examined the localization and concentration of reducible protein thiols, staining was exclusive to germinal center macrophages and sinus histiocytes. When we applied this technique to excisional lymph node biopsies diagnosed as involved by DLBCL, we observed a robust concentration of free protein thiols within the malignant cells that was comparable to the staining observed in benign germinal center cells. When we examined the localization and concentration of reducible protein thiols, we observed that in contrast to the benign tissue, the malignant cells demonstrated pronounced and diffuse staining.

Conclusions: We describe a novel and reproducible histochemical method for detecting protein thiols in-situ. In addition, we present the first in-situ data examining the distribution and concentration of free and reversibly oxidized protein thiols in high grade lymphoma specimens. Taken together, our findings demonstrate tissue thiols as a novel biomarker for further defining tumor histopathology.

2117 From HER2 FISH to DISH

R Alabdulghani, S Done, B Youngson, N Miller, H Berman, AM Mulligan, E Torlakovic, K Craddock. University of Toronto, Toronto, ON, Canada.

Background: In our institution HER2 status is assessed on all newly diagnosed breast cancers. HER2 FISH is performed on cases equivocal by immunohistochemistry (4B5 and SP3 clones). Dual in situ hybridization (DISH), an alternative to FISH, has advantages that include the use of light microscopy and slides can be archived and retrieved indefinitely.

Design: We performed HER2 DISH on a Benchmark Ultra (Ventana Medical Systems Inc., Roche) on 91 samples with equivocal IHC results that had previously been assessed by HER2 FISH (Pathvysion, Abbot). DISH was not interpretable in 1 case (technical failure), 7 cases were excluded; 6 due to clustered heterogeneity, and one had insufficient tissue. DISH was assessed by a breast pathology fellow and breast pathologists for inter-observer reproducibility. DISH was compared to FISH results obtained by two cytogenetics technologists.

Results: The fellow and pathologists had complete agreement between the FISH and DISH (positive, negative or equivocal) in 77% cases with no major discrepancies (positive vs negative). Minor discrepancies (negative vs. equivocal; or equivocal vs. positive) occurred in 22.9% of cases. HER2/CEP 17 ratio was≥1.6 in 0% of cases with major discrepancy and in 77% with minor discrepancy. The inter-observer agreement between DISH and FISH was not significantly different. DISH cases with ratios <1.6 or >2.2 showed 98% concordance of results with FISH. We have incorporated our results into practice as follows: DISH ratios <1.5 or >2.5 can be reported after counting a minimum of 20 nuclei. Ratios between 1.5 and 2.5 require counting of an additional 20 nuclei. If the ratio remains 1.6 to 2.2, an additional score by another observer is obtained. FISH is currently being performed within this range as well to gather more data within this range. We plan to re-evaluate this testing algorithm over time to optimize efficiency of HER2 testing.

Conclusions: HER2 DISH appears comparable to FISH. Major discrepancies between DISH and FISH results can be minimized by ensuring a second scorer within the ratio of 1.6 to 2.2.

2118 Comparison of C-Met Immunoreactivity in Surgically Treated Gastroesophageal Adenocarcinoma Using Two Commercially Available Antibodies

A Alkhasawneh, E Chan, T Zuluaga Toro, X Lu, S Hughes, T George, LV Duckworth. University of Florida, Gainesville, FL.

Background: C-met, hepatocyte growth factor (HGF) receptor, overexpression is known to be associated with tumor progression in lung, colon, and stomach carcinomas. Many ongoing trials are investigating c-met targeted therapy in these patients. In gastroesophageal adenocarcinoma (GEA), c-met is thought to confer resistance to anti-Her2 therapy. Currently, no guidelines exist as to interpretation of c-met immunohistochemistry (IHC) in GEA. The aim of our study was to compare c-met immunoreactivity in GEA using 2 commercially available antibodies and examine its relation to clinical outcomes.

Design: 48 cases of treatment-naïve GEAs were assessed for c-met expression using Ventana SP44 monoclonal antibody (prediluted/antigen retrieval with CC1 solution) and Leica NCL-CMET monoclonal antibody (1:80 dilution/antigen retrieval with Citra solution). Appropriate controls were evaluated. C-met membranous and/or cytoplasmic reactivity was graded as follows: 0=absent, 1=weak, 2=moderate, 3=strong and percent positive tumor cells was also recorded. Cases with <2+ or 30% staining were considered negative, and cases with≥2+ and 30% staining were considered positive. In addition, clinicopathologic features of GEAs were recorded.

Results: Median age was 66 yrs (range 37-83), with a 4:1 M:F ratio. Barrett's esophagus was seen in 92% of cases. Most GEAs (37/48) were low stage (T1-T2), and 10 had nodal involvement (N1/N2). The overall death rate was 33%. Positive staining was observed in 27 patients using either antibody; however, the concordance of positive cases using both antibodies was 16/27. The only variable that correlated significantly with survival was tumor stage (p = 0.007).

Conclusions: Our study demonstrates that caution must be exercised when assessing c-met status in GEA using different commercial antibodies. Pathologists and oncologists alike should be aware of the potential differences in staining that may impact treatment plans.

Analysis of c-met positive GEA using 2 different antibodies

	Ventana + cases (n=27)	Leica + cases (n=27)
Stage T1/T2	21	20
Stage T3/T4	6	7
Lymph node metastasis (N1/N2)	6	6
Recurrence	3	4
Deceased	10	11

22 Discrepant cases of c-met expression in GEA

	Ventana + but Leica – (n=11)	Leica + but Ventana – (n=11)
Stage T1/T2	9	8
Stage T3/T4	2	3
Lymph node metastasis (N1/N2)	2	2
Recurrence	2	3
Deceased	3	4

2119 Automated 3D Reconstruction of Digital Pathology for Registration to 3D Imaging

M Alturkustani, A Khan, JD Spence, M Cocker, C Crukley, L Hammond, C Lum, B Robert, J-C Tardif, T Peters, R Hammond. Western University, London, ON, Canada; Ottawa Heart Institute, Ottawa, ON, Canada; Robart's Research Institute, London, ON, Canada; Montreal Heart Institute, Montreal, PQ, Canada.

Background: Whole slide scanning opened new avenues for large-scale image analyses of pathological sections in clinical practice and research. Coupled with special stains, immunohistochemistry and manual or electronic annotations, digital images host a great deal of data. While images and data can be quickly acquired in 2D, an increasingly common goal is to acquire a 3D rendering of the pathology and a high resolution gold standard for imaging studies of the same.

Design: A goal of the Canadian Atherosclerosis Imaging Network is to develop improvements in imaging of carotid atheromas through comparative studies with excised plaque specimens. Sectioned atheromas are to be manually annotated for regions of interest (lipid core, calcification, etc.) and analyzed by electronic algorithms (eg. colorimetry of antigen expression). These semi-serial images are then to be reassembled in 3D for registration to in-vivo and ex-vivo ultrasound, CT, PET-CT and MRI.

Results: Recruited patients underwent carotid endarterectomy. Fixed plaque specimens were semi-serially sectioned, stained, scanned then annotated manually and with electronic algorithms. Resulting 2D images were then rendered in 3D in an automated fashion using ex-vivo micro-CT as a spatial reference for the individual slices.

Conclusions: Reconstruction of the pathology in 3D is greatly facilitated by this methodology in comparison to manual slice-by-slice methods. Since slice transforms are guided by a pre-existing model (micro-CT) the reconstruction is not only faster, but has greater objectivity and fidelity. With embedded annotations, the resulting 3D map contains abundant qualitative and quantitative data for such studies.

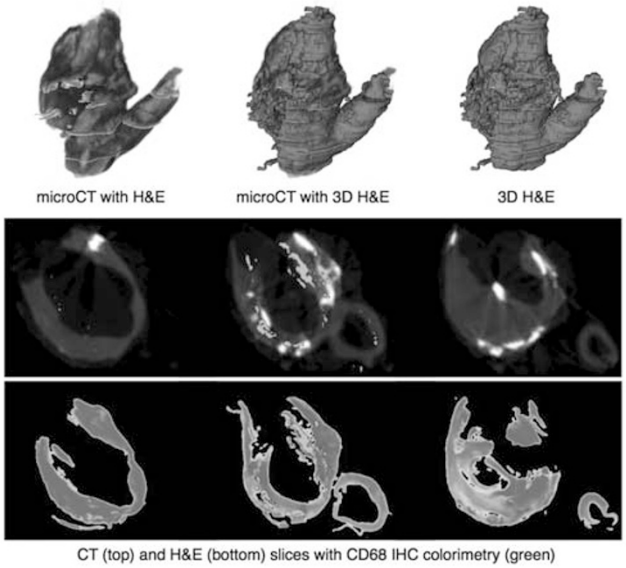

CT (top) and H&E (bottom) slices with CD68 IHC colorimetry (green)

2120 Quantitative Imaging of Ten Markers in Human Breast Tumors Using Multiplexed Ion Beam Imaging (MIBI) and Metal-Tagged Antibodies

M Angelo, SC Bendall, R Finck, M Hale, C Hitzman, AD Borowsky, RM Levenson, JB Lowe, SD Liu, S Zhao, Y Natkunam, GP Nolan. Stanford University, Stanford, CA; University of California Davis, Davis, CA; Genentech, South San Francisco, CA.

Background: Existing immunohistochemical (IHC) methods use antibodies tagged with fluorophores or enzyme reporters exhibiting significant spectral and spatial overlap when used simultaneously. Consequently, the advantages of highly multiplexed IHC are not routinely available in clinical settings. To circumvent these obstacles we have developed a novel method that images multiple mass-tagged antibodies using secondary ion mass spectrometry.

Design: Multiplexed ion beam imaging (MIBI) employs primary antibodies coupled to isotopically enriched, stable lanthanides. Tissue sections are stained simultaneously with all primary antibodies, then imaged using a NanoSIMS 50L mass spectrometer. In this study, multiplexed staining for ER, PR, & Her2, as well as e-cadherin, Ki67, keratin, vimentin, actin, and dsDNA was performed on human FFPE breast tumors and compared with conventional immunoperoxidase staining.

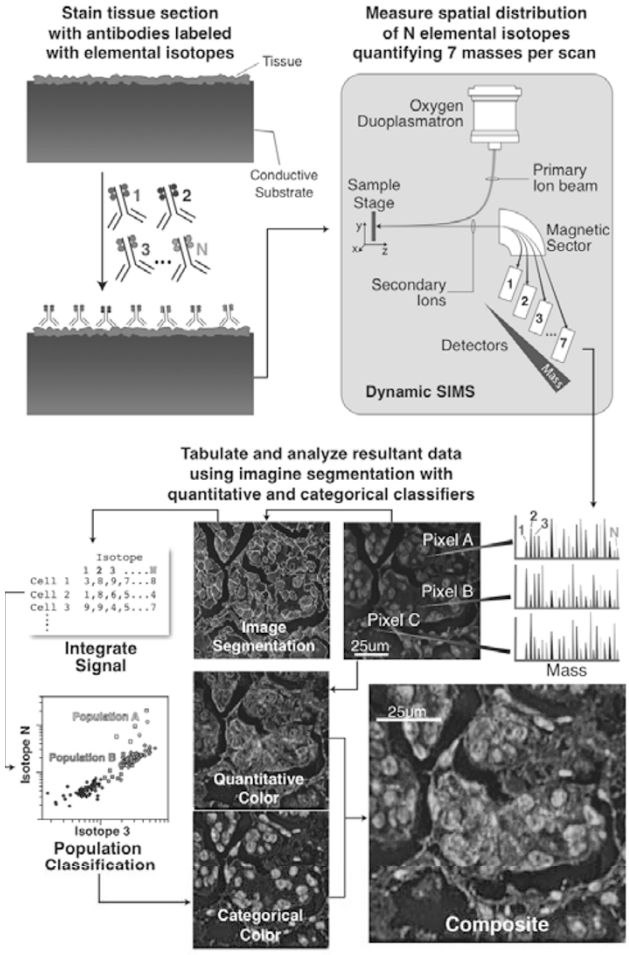

Results: Comparison of HER2-, ER-, and PR-positivity demonstrates appropriate expression with respect to immunophenotypes established by conventional IHC staining performed in a clinical lab. Side-by-side comparison of MIBI and quantitative imaging analysis (QIA) of ER IHC in nine breast tumors demonstrated robust agreement between the two methods with respect to mean nuclear staining intensity and H-score ($r = 0.99$ $p < 0.00001$ and $r = 0.99$, $p < 0.00001$, respectively).

Conclusions: MIBI analysis can be used for highly multiplexed imaging applications with sensitivity and resolution comparable to conventional IHC methodologies. These data indicate that MIBI can integrate tissue microarchitecture with multi-parameter expression patterns, thus enabling new histopathological insights of relevance to basic research, drug discovery and clinical diagnostics.

2121 Clinical Validation of *IDH1 & IDH2* Mutation Detection in Formalin-Fixed Paraffin Embedded Glioma Tissues

K Arora, JR Lindner, EM De Leon, JM Henry, K Vadlamudi, JM Osman, J Jagirdar, WB Furmaga, H Fan. University of Texas Health Science Center, San Antonio, TX.

Background: Mutations in isocitrate dehydrogenase 1 and 2 (*IDH1* & *IDH2*) genes have been identified in gliomas, predominantly in low-grade and secondary high-grade gliomas. These mutations can be used as a diagnostic and prognostic marker. We evaluated the IDH1 & IDH2 mutation status in routine formalin-fixed paraffin-embedded (FFPE) glioma tissues, utilizing the Sanger DNA sequencing method.

Design: A hospital database search was performed for cases of glioma diagnosed between 2005-2013. A total of 52 gliomas were identified; 2 biopsy cases were excluded due to poor DNA quantity, resulting in 50 gliomas for analysis, including: 11 WHO grade I (10 pilocytic astrocytomas, 1 myxopapillary ependymoma); 10 WHO grade II (2 astrocytomas, 2 ependymomas, 5 oligodendrogliomas and 1 oligoastrocytoma); 7 WHO grade III (5 anaplastic astrocytomas, 1 anaplastic ependymoma, 1 anaplastic oligodendrogliomas); and 22 WHO grade IV glioblastomas (GBM). Patients ranged from 2-75 years of age (median 46); 31 were males and 19 females. DNA was directly extracted from FFPE sections by the EZ1 DNA Tissue Kit (Qiagen) without macrodissection; estimated tumor cells on the paraffin section ranged from 20-100% (median 80%) and DNA yield ranged from 6-187ng/ul (median 23). DNA was then amplified by primers targeting the IDH1 codon 132 and IDH2 codon 172 regions, and sequencing was performed bi-directionally on the ABI3130xl Genetic Analyzer (Applied Biosystems). The assay is sensitive to detect 25% mutant (MT) allelein the specimen. The relative percentage of MT allele in the sample was estimated by comparing maximum height between mutant and wild type peaks on the sequencing eletcropherogram.

Results: Mutations were not detected in 7 pilocytic astrocytomas of children. The IDH1 R132H mutation was detected in 11 adult gliomas, including: 1/4 (25%) WHO grade I; 5/8 (63%) WHO grade II; 3/6 (50%) WHO grade III; and 2/21 (9.5%) WHO grade IV. The relative quantities of the R132H allele ranged from 25-51% (median 39%). In addition, the IDH2 R172M mutation was detected in one WHO grade II oligodendroglioma. Three WHO grade II oligodendrogliomas with chromosome 1p19q codeletions were characterized by either IDH1 or IDH2 mutation. Among 12 positive cases, there was a male predominance (8/12 male, 67%).
Conclusions: Our results indicate that, using Sanger sequencing method, IDH1 & IDH2 mutations can be effectively detected in routine FFPE samples. The detected MT allele levels below 50% suggest that most glioma cells carry heterozygous mutations. These findings replicate data published in the pertinent literature.

2122 Fixative Comparison Study of MMR Assessment by IHC: Clear Superiority of formalin Fixation over Other Fixatives

H Bailey, C Millward, S Michelson, FL Baehner. Genomic Health, Inc, Redwood City, CA; University of California, San Francisco, San Francisco, CA.
Background: Preserving clinical patient tissue specimens as fixed, paraffin-embedded (FPE) tissue is standard practice in hospital pathology laboratories. However, the methodology for tissue fixation is not standardized and alternative fixatives are commercially available. Non-formalin fixatives can produce H+E slides with high-quality staining. However, antigen immunoreactivity may vary and may not produce the same patterns seen in formalin-fixed tissue. Few direct comparisons of immunohistochemistry (IHC) results between formalin-fixed and non-formalin-fixed tissue have been performed. Here we compare IHC results for mismatch repair proteins MLH1 and MSH2 in non-formalin fixed tissues to results in formalin-fixed tissue.
Design: IHC was performed on a series of archival paraffin-embedded placenta tissue blocks from a single specimen. Nine fixatives (B5, Bouin's, ethyl alcohol 70%, formalin, Hollande's, Pen-fix, Prefer, Zenker's, & zinc formalin) were compared. IHC assays were performed on the Leica Bond III Automated IHC system following optimized protocols for each antibody and were scored using a semi-quantitative method. The slides were randomized, stained, and read by a pathologist blinded to fixative. IHC staining and assessment for MLH1 (ES05,Leica) and MSH2 (G219-1129,Cell Marque) were categorized into 0, 1+, 2+, and 3+ results by comparing the intensity of nuclear staining in the test samples to that observed in the formalin-fixed control tissue.
Results: IHC assays demonstrated variation across the different tissue fixatives (Table 1). All fixatives except one (zinc formalin) showed reduced staining intensity compared to formalin-fixed positive control. No fixative-induced non-specific staining on negative reagent control slides was observed for any of the non-formalin fixatives.
Conclusions: Pre-analytic effects of tissue fixation can dramatically influence the immunoreactivity of MLH1 and MLH2 IHC antibodies. Most non-formalin fixatives were associated with decreased expression when compared to formalin positive control. These findings must be taken into consideration when evaluating IHC on non-formalin-fixed samples and they support the uniform use of formalin as a fixative for IHC.

Table 1. Staining Intensity Scores by Fixative

	MLH1 Staining (# of blocks)				MSH2 Staining (# of blocks)				Negative Reagent Control	Total # of Blocks
Fixative	0	1+	2+	3+	0	1+	2+	3+	Pass	
B5			2			2			2	2
Bouin's			2			2			2	2
Ethyl Alcohol 70%		2			2				2	2
Formalin				10				10	10	10
Hollande's		1	1			2			2	2
Penfix			1	1		1	1		2	2
Prefer	1	1			1	1			2	2
Zenkers		4			4				4	4
Zinc Formalin				2				2	2	2

2123 Protease Activity Analysis and Pathologic Examination on the Same Endoscopic Biopsy Specimen in Inflammatory Bowel Disease

WW Bivin, C Falco, SD Finkelstein, K Clarke, JF Silverman. Allegheny General Hospital, Pittsburgh, PA; Carnegie Mellon University and Enzium, Inc, Pittsburgh, PA.
Background: Inflammatory bowel disease (IBD) is characterized by an inflammatory infiltrate associated with architectural changes along with an increased turnover of extracellular matrix components. Matrix metalloproteinases (MMP) are the most important group of proteolytic enzymes responsible for extracellular matrix breakdown in IBD. MMPs have been shown to correlate with IBD severity, and protease activity (PA) levels may help differentiate Crohn's disease (CD) from ulcerative colitis (UC). Biomarker assays often compete with histopathology for the same tissue. We developed a technique to assay MMP activity levels and perform histopathology on the exact same mucosal biopsy while preserving histologic integrity.
Design: Following patient consent, 15 endoscopic mucosal biopsies (6CD, 9UC) sampled *in vivo* from IBD colon and terminal ileum were immediately placed in 1 mL of isotonic saline and incubated at room temperature for 2 hours. Following incubation, the biopsies were transferred to formalin and processed for histopathologic evaluation. The saline was retained and 25 microL was assayed against a panel of fluorogenic reagents for the detection of PA for 3 MMP markers involved in inflammation. The fluorescent signal was recorded every 2 minutes for 120 minutes, and average fluorescent signal output was calculated for each data point. The percent increase in fluorescent signal was calculated using background adjusted averages of protease detection reagent with and without incubated solution [(Bx Signal 120m)–(Neg Control Signal 120m)]/(Neg Control Signal 120m). Based on previous validation studies, an increase in signal >20% over background signal was considered a significant increase in PA.
Results: The mean percent increase in PA level is significantly higher in CD compared to UC for all 3 proteases tested. The mean percent signal increase in CD vs. UC samples were 272.5% vs. 88%, 29% vs. 3.3%, and 123.7% vs. 25.1%, respectively. Histopathology using routinely processed FFPE tissue following saline incubation was satisfactory for pathologic interpretation.
Conclusions: The extracellular PA level can be measured in the exact same IBD mucosal biopsies sampled for pathologic evaluation while maintaining histologic integrity and can provide useful complementary information for the histologic differentiation of CD-related colitis and UC.

2124 Quantitative Assessment of Her2 Using Molecular Inversion Probe Arrays in Patients with High Grade Tumors Expressing Her2 Amplification by FISH

A Bousamra, R Luthra, X Lu, KD Aldape, AA Sahin, RR Singh, G Lu, R Abraham. MD Anderson Cancer Center, Houston, TX.
Background: A variety of methods are available for assessing Her2 status in solid tumors using formalin-fixed paraffin-embedded (FFPE) tissue, with Her2 amplification ratios by fluorescence in situ hybridization (FISH) and overexpression by immunohistochemistry the most widely used. Due to challenges encountered in FFPE samples, Her2 status is mostly assessed qualitatively. However, with the advent of different types of anti-Her2 therapy, quantitative Her2 evaluation is becoming an important clinical need. Recently, molecular invasion probe (MIP) technology (Affymetrix, Santa Clara, CA) has proven capable of generating high-quality copy number data in FFPE samples, requiring minimal DNA. We applied MIP technology on different FFPE tumor samples displaying Her2 amplification by FISH to assess the applicability of the platform for Her2 copy number analysis.
Design: Ten high grade tumors exhibiting Her2 amplification by FISH (Invasive ductal carcinoma of the breast, N=8; Endometrial adenocarcinoma, N=1; Salivary gland carcinoma) were selected from the archives of MD Anderson Cancer Center. For each tumor, 5 um thick sections were cut from a representative FFPE tissue block. After manual microdissection, DNA was extracted using PicoPure DNA extraction kit (Arcturus, Mountain View, CA). DNA samples (80 ng) were subjected to genome-wide copy number estimation using the OncoScan MIP array and Her2 copy number data were analyzed using Nexus Express Software7.0 (Biodiscovery, Hawthorne, CA).
Results: All ten selected patients (Average age: 51) expressed Her2 amplification by FISH (Signal ratio range: 2.35-8.57). Immunohistochemical staining for Her2 was performed in six cases (60%), with five of them showing overexpression (3+) and one equivocal result (2+, FISH signal ratio: 2.35). All ten samples submitted for MIP array processing showed Her2 (chromosome 17q) copy number gains. "High copy number (CN) gain" was reported in seven samples (70%) (Breast, N=5, Endometrium, N=1, Salivary gland, N=1), and "CN gain" in three cases (30%) (Breast, N=3).
Conclusions: All ten high grade tumors selected for our study expressed Her2 copy number gains by MIP array technology, correlating well with their amplified Her2 status by FISH. With only minimal DNA concentration requirements using FFPE tissue, MIP array technology allows for a more accurate representation of the patient's tumor's Her2 status by providing clinicians with quantitative values, and thus a better guidance in their clinical decision in regards to anti-Her2 therapy.

2125 *FGFR1* Dual-Color Chromogenic and Silver In-Situ Hybridization – A New Tool for the Detection of the *FGFR1* Copy Number Status

M Braun, D Boehm, W Vogel, A Schrock, F Bootz, LE Heaseley, S Perner. University Hospital Bonn, Bonn, Germany; University of Colorado at Denver, Aurora, CO.
Background: Recently, the fibroblast growth factor receptor 1 (*FGFR1*) was described as the first actionable target in squamous cell lung cancers. Clinical trials testing specific FGFR inhibitors are in process and patients are selected based on their *FGFR1* copy number status. Fluorescence in-situ Hybridization (FISH) is the most commonly used method for detecting *FGFR1* amplifications, but it has its limitations. Here, we established a new long lasting and easily assessable *FGFR1* chromogenic and silver in situ hybridization (CS-ISH) assay.
Design: We assessed 394 patients diagnosed with head and neck squamous cell carcinoma with the *FGFR1* CS-ISH assay and compared these results with those obtained by *FGFR1* FISH.
Results: The FISH assay was assessable in 86.8% (342/394) of cases, whereas the CS-ISH was successful in 79.4% (313/394) of cases. *FGFR1* amplification was detected by FISH in 12.6% (43/342). In detail, 7.6% (26/342) showed a low level amplification (LLA) and 5.0% (17/342) a high level amplification (HLA). 87.7% (317/351) of our investigated specimens displayed no *FGFR1* amplification. By CS-ISH, 10.2% (32/313) showed an amplification. In detail 5.7% (18/313) showed a LLA, 4.5% (14/313) a HLA

and 89.8% (281/313) of our investigated specimens displayed no *FGFR1* amplification. A high concordance (Pearson´s correlation coefficient= 0,971, $p < 0.01$) was observed comparing both techniques.

Conclusions: The ease of bright field microscopy, fully automated workflow, oil free evaluation and stable, light-insensitive signals are features that open up CS-ISH based *FGFR1* amplification assays for the widespread use in clinical routine and research laboratories. Hence, we emphasise CS-ISH as a new tool for the identification of gene amplifications.

2126 Comparison of Proliferation Markers Ki-67 and Phosphohistone-H3 (pHH3) in Ductal Carcinoma In Situ of Breast

OH Chang, MR Kilgore, RA Schmidt, PE Swanson, MH Rendi. University of Washington Medical Center, Seattle, WA.

Background: There is emerging interest in ascertaining the proliferative rate of ductal carcinoma in situ (DCIS) of breast and the relationship to recurrence risk and/or progression to invasive disease. However, it can be difficult to determine an accurate proliferative rate using conventional methods. Searching for mitotic figures on H&E-stained sections can be problematic; especially in finding rare mitotic cells and differentiating between mitosis versus nuclear karyorrhexis/pyknosis. Ki-67 is the most commonly used immunohistochemical stain for estimating proliferative index by marking interphase and mitotic cells. Pitfalls of Ki-67 include variation in staining intensity threshold of positivity, and inter-/intraobserver variance in percentage estimation, making proliferation estimates unreliable. Phosphohistone-H3 (pHH3) is a novel immuno-marker which binds the phosphorylated form of histone H3, present only during mitosis. Our aim is to assess the performance characteristics of pHH3 in DCIS using Ki-67 as the gold standard as a basis for more formal assessment of proliferative activity.

Design: 23 patients with an initial diagnosis of DCIS were selected and immunohistochemistry for Ki-67 and pHH3 was performed on the corresponding slides. 1000 cells were counted from each case in areas of DCIS with the highest proliferative activity. Any nuclear staining was considered positive for both stains.

Results: There is a strong, positive linear relationship between quantitative immunohistochemical assessments of Ki-67 and pHH3 ($p<0.0001$, $r^2=.8878$). pHH3 stain intensity was generally more uniform than that observed for Ki67. Variations in the intranuclear distribution of pHH3 reactivity mirrored the light microscopic appearance of mitotic phase, whereas Ki-67 stains were inhomogeneous

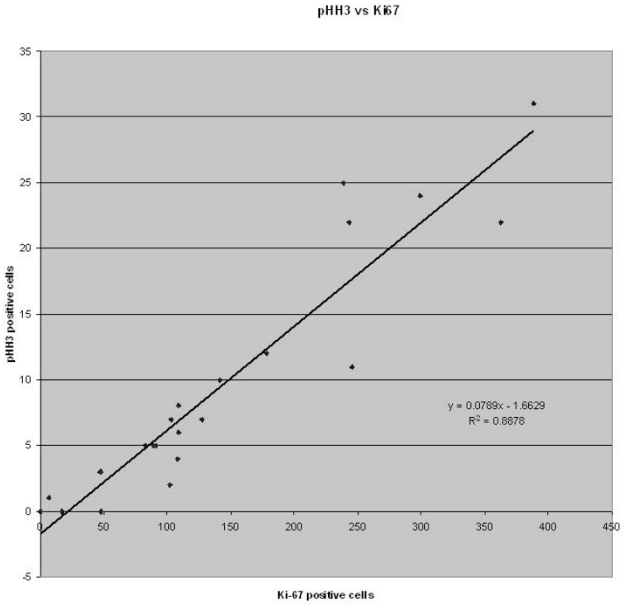

Conclusions: The strong correlation between pHH3 and Ki67 confirms the relative utility of this marker as a measure of proliferative activity in DCIS. The stain quality across positive nuclei suggests that pHH3 provides a more reproducible light microscopic measure of proliferation than Ki-67, and the morphologic overlay of pHH3 and mitotic phase reinforce the utility of pHH3 as a surrogate for directly assessing mitotic activity.

2127 Confocal Laser Endomicroscopy (pCLE) Improves Diagnostic Material Obtained by Bronchoscopy: Comparison of pCLE Pulmonary Images with Surgical Biopsies for Lung Cancer Diagnosis

CS Chaudoir, LH Brandi, AS Wellikoff, RC Holladay, EA Turbat-Herrera. LSU Health Sciences Center, Shreveport, LA.

Background: Probe-based confocal laser endomicroscopy (pCLE) is a new FDA approved tool used for in vivo microscopic imaging of proximal and distal airways including bronchial and alveolar walls, microvessels, and inflammatory cells. Light at 488nm wavelength is focused via a pinhole-sized aperture incorporated into a flexible probe that fits into the working channel of a standard bronchoscope and reflected back through that aperture to produce an image that can aid in the identification of neoplastic processes. Studies have demonstrated elastin and collagen fibers as having endogenous fluorescence by pCLE. No studies have correlated in vivo imaging by pCLE to pathologic samples obtained during bronchoscopy. This combination could prove diagnostically advantageous to both clinician and pathologist.

Design: 24 patients have been studied by pCLE and compared to biopsies from 7/17/12 and 1/28/13. pCLE and bronchoscopy were employed to help determine abnormal bronchial or alveolar changes. We correlated pCLE images with biopsies obtained during bronchoscopy. Patients ranged from 47 to 82 years of age (14 males, 10 females). 25 biopsies included 11 adeno, 8 squamous, 4 poorly differentiated carcinomas and 2 "other" (1 small cell and 1 metastatic).

Results: By pCLE, differences between normal, inflammation and neoplasia can be viewed. Normal findings consist of organized connective tissue fibers. Inflammatory cells, mostly macrophages, can be recognized within tissue spaces. In neoplastic tissue, a ragged surface can be observed along with disorganization of the collagen/elastin fibers within the bronchus/alveoli. Differences between squamous (SCC) and adenocarcinomas (ADC) can be suggested on the basis of imaging patterns. SCC shows friability and dense areas of auto fluorescence with "dark spots" representing tumor groups. ADC shows less fluorescence and tumor appears as "black holes" giving a mottled appearance. ADC with bronchioloalveolar differentiation and a lepidic pattern of growth can be suspected when a "studded appearance" is noted. Disarray of fibers increases with more poorly differentiated carcinomas. Biopsies and pCLE images can be correlated by using tissue patterns.

Conclusions: pCLE allows the distinction between benign and malignant tissues, assists in obtaining diagnostic tissue, and recognizes tumor growth patterns. Correlation between biopsies and pCLE can help aid sampling and diagnostic techniques. Larger studies can enhance our understanding of how pCLE can help differentiate tumor types.

2128 Clinical Validation of Tumor Specific Panels for Melanoma and Gastrointestinal Stromal Tumor by Next Generation Sequencing

G Chen, S Mosier, A Pallavajjalla, M-T Lin, JR Eshleman, CD Gocke. Johns Hopkins University School of Medicine, Baltimore, MD.

Background: Next generation sequencing (NGS) technology is becoming a cost-effective and potentially major sequencing platform for clinical diagnostic laboratories. One feasible approach to implement NGS testing for oncology is offering gene panels by sequencing targeted regions with known mutations clinically important for specific types of tumor.

Design: Accordingly, we built a tumor specific panel for melanoma including *BRAF, KIT, NRAS* and *PIK3CA* genes and one for gastrointestinal stromal tumor (GIST) including *KIT* and *PDGFRA* genes from the Ion AmpliSeq Cancer Hotspot Panel using the Ion Torrent Personal Genome Machine. Given that validation of *NRAS*, *BRAF* and *PIK3CA* genes has previously been done, in this study we completed the process by validating detection of *KIT* and *PDGFRA* gene mutations. In addition to a cell line harboring a known *KIT* mutation and a clinical sample with a documented *PDGFRA* mutation as positive control, and 4 peripheral blood samples from healthy donors and 16 formalin-fixed paraffin-embedded (FFPE) lymph node specimens from patients without known neoplastic diseases as negative control, 36 tumor FFPE samples were tested for *KIT* and/or *PDGFRA* mutations by NGS and Sanger sequencing.

Results: All the control samples were demonstrated by NGS correctly. NGS detected *KIT* mutations in 20 out of 21 tumor specimens confirmed by Sanger sequencing. The one missed by NGS carries a 48-base duplication mutation and was revealed by a capillary electrophoresis length assay that was designed to detect indel mutations in exon 9 and exon 11 of the *KIT* gene. NGS identified 3 out of 3 specimens with known *PDGFRA* mutations. In the 15 tumor specimens that were reported as wild type by Sanger sequencing, NGS detected *KIT* mutations in two of them at a frequency below the limit of detection of Sanger sequencing. Mutant allele frequencies in the positive FFPE tumor specimens ranged from 5% to 90% for *KIT* mutations, and 33% to 97% for *PDGFRA* mutations. It was demonstrated that adequate depth of coverage for a 5% (mutant allele frequency) limit of detection is >500X, and for 10% limit of detection is >150X. Also, analytic precision, reportable range and reference range were determined.

Conclusions: In conclusion, offering a melanoma panel including *BRAF, KIT, NRAS* and *PIK3CA* genes and a GIST panel including *KIT* and *PDGFRA* genes by NGS is clinically practical.

2129 Heat-Induced Cytosine Deamination Contributes to Baseline Noise in Next Generation Sequencing

G Chen, S Mosier, M-T Lin, CD Gocke, JR Eshleman. Johns Hopkins University School of Medicine, Baltimore, MD.

Background: Next generation sequencing technology is revolutionizing molecular research and medical practice, and becoming a major sequencing platform in clinical diagnostic laboratories. In addition to detecting gene mutations for cancer diagnosis and prediction of treatment response, it can be potentially used for the early detection of cancer or monitoring minimal residual diseases due to its superior sensitivity. Consequently, it is critical to correctly identify and interpret reproducible sequence artifacts generated during NGS because they constitute baseline noise of sequencing data and may interfere with detection of true gene mutations.

Design: In a recent study of validating detection of gene mutations by next generation sequencing, we evaluated background noise by checking all common KRAS (codons 12 and 13), BRAF (V600E) and EGFR (T790M and L858R) gene point mutations in wild type peripheral blood and formalin fixed paraffin embedded samples.

Results: We observed significantly higher rates of C:G > T:A mutations than other background noise in both types of samples. Treating peripheral blood samples with uracil DNA glycosylase significantly reduced the C:G > T:A mutations, which further supports our interpretation that this baseline noise is due to deamination, manifesting as either C>T or G>A mutations on the sense strand. To test whether heat during

thermocycling can contribute to the deamination mutation, we thermocyled the samples as a Pre-PCR step and found that the extra heat significantly increased the rate of C:G > T:A mutations without affecting other baseline base changes.
Conclusions: In conclusion, baseline noise during next generation sequencing is associated with cytosine deamination, which may be elevated by heat during thermocycling and reduced by uracil DNA glycosylase.

2130 Diagnostic Usefulness and Limitations of Endoscopic Ultrasound Fine Needle Aspiration Cytology (EUS-FNAC) in a Series of 428 Pancreatic Lesions

A Corominas-Cishek, A Perez, A Barturen, I Casado, JA Alvarez, L Mosteiro. Cruces University Hospital, Barakaldo, Bizkaia, Spain.
Background: To describe the usefulness and limitations of EUS-FNAC in the diagnosis of pancreatic lesions.
Design: EUS-FNAC was performed in 428 pancreatic lesions during a 6-year period (2007-2012) at the Cruces University Hospital, Barakaldo, Spain, by the same team of endoscopists and pathologists. Cytological diagnoses were correlated in 106 cases (24.7%) with the histological diagnoses made on subsequent core biopsies or surgical specimens. Clinical and radiological follow-up served as control in the 322 cases (75.3%) in which surgery was not performed. Additionally, the accuracy of this diagnostic technique depending on the presence or absence of the pathologist in the endoscopy room was compared.
Results: One hundred and twenty-five adenocarcinomas (29.2%), 19 neuroendocrine tumors (4.3%), 13 mucin-producing neoplasms (3%), 3 solid-papillary tumors (0.7%), 1 malignant lymphoma (0.2%) and 19 lesions suspicious of malignancy (4.3%) were diagnosed on cytological smears. Two hundred and thirteen cases were diagnosed as negative for malignancy (49.7%) and 35 (8.17%) yielded inconclusive results due to scarce cellularity or to highly haemorrhagic smears. After cyto-histological correlation or clinico-radiological follow-up, 178 cases were considered true positive (45.2%), 167 true negative (42.4%), 2 false positive (0.5%) and 46 false negative (11.7%). Sensitivity, specificity, and positive and negative predictive values were 79%, 98%, 98% and 78%, respectively. Roughly half of the false negative cases were related to the intrinsic characteristics of the lesion. Among them, the most frequent were cystic (72.3%), haemorrhagic (13.6%) or badly delimited (13.6%) lesions. When the pathologist was present at the endoscopy room while the procedure was performed, the rate of non diagnostic smears decreased from 16% to 8% ($p<0.015$).
Conclusions: EUS-FNAC is an efficient diagnostic technique in pancreatic lesions, although cystic lesions remain a challenge for pathologist and the main source of false negatives. Best results are obtained with the pathologist present in the endoscopy room while performing the technique.

2131 Profiling microRNA Using Locked Nucleic Acid Q-rtPCR in Formalin Fixed Tissue and Plasma

DL Duncan, AL Treece, W Tang, SC Kenney, N Raab-Traub, ML Gulley. University of North Carolina at Chapel Hill, Chapel Hill, NC; University of Wisconsin, Madison, WI.
Background: Expression profiling of microRNA (miRNA) may be valuable in classifying disease and in monitoring disease burden. To be applicable in clinical settings, traditional Q-rtPCR has advantages over other miRNA technologies, especially given commercial availability of plates pre-loaded with lyophilized, custom primer sets. Additionally, newly developed locked nucleic acid (LNA) technology may enhance sensitivity and specificity beyond traditional Q-rtPCR.
Design: We examined the utility of Exiqon's LNA technology for miRNA Q-rtPCR on practical clinical specimen types including macrodissected formalin-fixed paraffin embedded (FFPE) tissue and plasma from gastric cancer patients and controls. A panel of 48 miRNA assays was designed to include 12 candidate normalizer miRNAs, 33 miRNAs having putative utility in gastric carcinoma or lymphoma diagnosis, and 3 controls. The assay was applied to 114 samples including 76 FFPE tissues, 18 FFPE cell line pellets, and 20 plasmas. Candidate normalizer miRNAs were evaluated using NormFinder and geNorm algorithms with Exiqon-GenEx software. Duplicate test results on all specimens were evaluated for reproducibility. Also, indicators of epithelial versus lymphoid lineage were examined in FFPE and tumor patient plasma.
Results: NormFinder and geNorm algorithms independently identified two stably expressed miRNAs (miR-191, miR-425) in both gastric tissues and plasma, suggesting that the same normalization technique could be used on both sample types to control for input amount and cDNA quality. Spiked miR was recovered, implying that plasma extraction, plasma or FFPE cDNA preparation, and amplification steps worked as expected. When comparing epithelial to lymphoid cell lines in FFPE samples, 24 miRNAs were dysregulated between the two lineages ($p<0.05$). Of these 24 miRNAs, 11 were also dysregulated when comparing epithelial and lymphoid cancer patient plasmas ($p<0.05$). As for reproducibility, duplicate measurements of miR-191 and miR-486-5p showed excellent correlation ($r=0.92$ and 0.98, respectively).
Conclusions: Our evaluation of multiple quality assurance parameters implies that LNA Q-rtPCR is robust for profiling miRNA expression in FFPE and plasma samples. Reproducible results obtained from common sample types using straightforward techniques bring us closer to creating miRNA assays for clinical implementation.

2132 BRAF Mutations in Metastatic Malignant Melanoma (MM): Comparison of Molecular Analysis (MA) and Immunohistochemical (IHC) Expression Using Two Different Antibodies

L Ehsani, C Cohen, KE Fisher, MT Siddiqui. Emory University Hospital, Atlanta, GA.
Background: Approximately 90% of BRAF mutations in MM involve a specific substitution at codon 600 (BRAF V600E). The second most common mutation is BRAF V600K, followed by BRAF V600R, an infrequent two-nucleotide variation of the predominant mutation, BRAF V600 'E2', and BRAF V600D. The sensitivity of detecting *BRAF* V600E by COBAS 4800 on fixed paraffin-embedded (FFPE) samples of MM is high. We compared BRAF (V600 E) mutation detection by MA with BRAF expression by IHC using two different antibodies.
Design: 25 cases of metastatic MM (19 excisional biopsies, 6 fine needle aspiration cell blocks [CB]) were included. BRAF V600 E mutations were detected using the COBAS® 4800 BRAF V600 Real-time PCR assay. IHC was performed with the Dako Autostainer, using i) a rabbit anti-BRAF monoclonal antibody (MAB, pan-BRAF, Abcam, Clone EP152Y, Cambridge, MA) raised against a synthetic peptide representing the common N-terminal amino acids 70-86 shared by both wild-type BRAF and BRAF V600E protein (1:20); and ii) a mouse anti-BRAF MAB (mut-BRAF, Spring Bioscience, Clone VE1, Pleasanton, CA) raised against a synthetic peptide representing BRAF V600E mutated amino acid sequence from amino acid 596 to 606 (1:40). IHC results were interpreted as positive if at least 10% of cells showed moderate cytoplasmic staining. Three pancreatic lesions were negative controls, and MA was the gold standard.
Results: 10/25 (40%) were positive by MA and 18/25 (68%) cases by IHC (Abcam and Spring). The results of the two antibodies were the same. All 10 positive cases by MA were positive by IHC (100%). No false negative and eight false positive cases, were obtained. All 3 negative controls were negative.

	Sensitivity	Specificity	PPV	NPV	Accuracy
IHC (Abcam)	100%	47%	56%	100%	68%
IHC (Spring)	100%	47%	56%	100%	68%

Conclusions: MA for the BRAF V600 E mutation in metastatic MM is an accurate and sensitive test. IHC yields a high sensitivity; however, the specificity is lower which may be due to the cross reactivity in the presence of other BRAF point mutations like V600K, V600R, V600 'E2' and V600D. IHC testing is less expensive, easier to perform, less time consuming and has a shorter turnaround time when compared to MA. Hence, it can be useful for initial screening evaluation of BRAF mutations in metastatic MM. MA can be supplemental for IHC positive or equivocal cases, resulting in cost containment. The Abcam antibody is cheaper than that from Spring, and may be more cost effective, although not directed at the V600E mutation.

2133 Direct Autofluoresence Visualization to Guide Breast Specimen Grossing: A Proof-of-Concept

S El Hallani, C Poh, S Hakim, P Lane, D Gravel, S Robertson, S Islam. The Ottawa Hospital, Ottawa, ON, Canada; BCCA, Vancouver, BC, Canada.
Background: Traditional gross examination of breast specimen relies on naked eye visualization in conjunction with palpation and radiologic correlation. In many situations; however, the lesion is occult and non-palpable due to the lack of surrounding desmoplastic response (i.e. DCIS; lobular carcinoma) or small tumor size (i.e. early cancer detection; area of invasion in DCIS). When practical, multiple cassettes are submitted in sequential fashion for in toto histological examination. This practice affects the tech-time and significantly increases the laboratory cost and the pathologist work-load. A simple method to identify such occult lesions is tested.
Design: A hand-held device that delivers blue excitation light was employed to induce green fluorescence from endogenous fluophores (i.e. collagen) in the extracellular matrix of the mammary fibrous tissue. Breakdown of the fluorescent collagen is observed in cancer invasion and stromal inflammation and lead to loss of normal autofluorescence (LOA). Ninety-five tissue sections taken from fifteen fixed Breast specimens during routine gross procedures were randomly selected and examined with the DAV device. Digital images of tissue white-light reflectance and fluorescence of the whole sections were saved and compared to the H&E slides of final pathology.

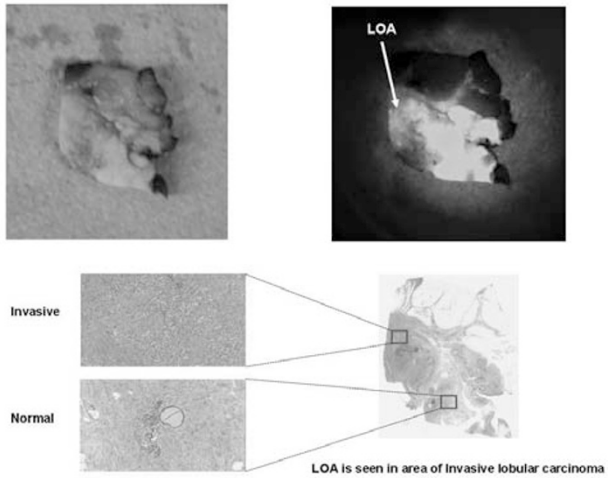

Results: Using histology as the gold standard, the device achieved a sensitivity of 100% when discriminating benign mammary conditions (n=49) from invasive ductal carcinoma (n=26) and lobular carcinoma (n=6). Comprehensive white light examination showed some invasive ductal carcinoma lesions; however, the addition of DAV was helpful in identifying the true extent of these lesions through the LOA. Biopsy site (n=5) showed also LOA in correlation with fat necrosis and surrounding stromal inflammation. Almost 85% of total DCIS lesions (n=9) appeared with a specific pattern of small round LOA areas that is different from the invasive pattern.

Conclusions: We believe that DAV technology has a potential application in guiding the gross examiner to perform targeted sampling and precise extent assessment of cancerous Breast lesions including the occult ones, setting a new standard in gross examination. Ultimately, this will save the tech-time and reduce the financial laboratory cost.

2134 The Effect of Decalcification Solutions on Kappa and Lambda In-Situ Hybridization

PE Ferguson, YM Sanchez. St. Bernards Medical Center, Jonesboro, AR; Arizona State University, Phoenix, AZ.

Background: Consistent reliable in-situ hybridization (ISH) staining on decalcified FFPE bone marrow biopsies has been a significant challenge. This study evaluates and compares decalcification cutting and kappa/lambda ISH staining characteristics of five decalcification solutions to identifying solution(s) with the best performance.

Design: Five random benign tonsils and one femoral head were decalcified for 0.5, 1, 2, and 4 hours in five separate decalcification solutions (Formical-2000*solution 1, Nitrical*solution 2, Formical-4* solution 3, EDTA*solution 4, and Immunocal*solution 5). Tonsil sections were stained for kappa and lambda by ISH (Novocastra). Stain characteristics were graded on blinded material, and compared to non-decalcified tonsil sections using Hierarchical Linear Model analysis. The femoral head was cored with a standard bone marrow core biopsy needle, and cutting adequacy was also evaluated at 0.5, 1, 2, and 4 hours. Specimens were blinded and judged as acceptable, cutting not optimal, or unacceptable by an experienced histotechnologist.

Results: Decalcification solutions Formical 2000, Formical 4, and Immunocal demonstrated approximately equivalent quality in staining (average score = 7.642, 7.952, & 7.805, respectively) through 4 hours. Nitrical and EDTA showed significant drop-off in stain performance (Figure 1). Four solutions had acceptable cutting performance at 1 hour of decalcification, but Immunocal was slower with adequate cutting obtained at 2 hours (data not shown).

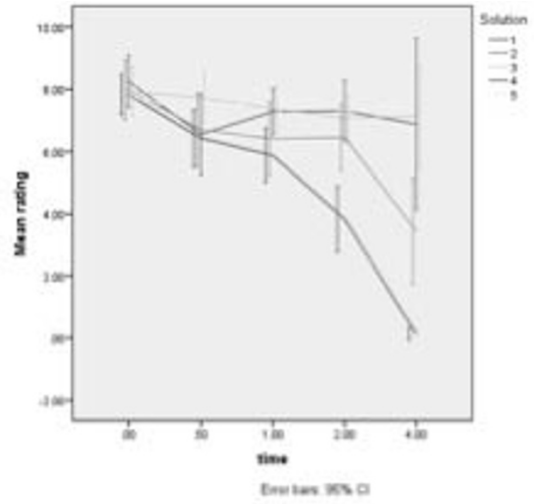

Conclusions: Formical-2000, Formical-4, and Immunocal demonstrated acceptable and similar staining performance. However, Immunocal required longer decalcification. These solutions should be considered as leading candidates for use in histology laboratories.

2135 Quantitative Assessment of Gaze Pattern and Specimen Presentation on Digital Platforms

SE Fox, CC Law, BE Faulkner-Jones. Beth Israel Deaconess Medical Center, Boston, MA; Kitware, Inc, Clifton Park, NY.

Background: In order to optimize diagnostic capability through digital means, it is important to understand the visual process by which pathologists arrive at image-based diagnoses. Eye-tracking systems enable the analysis of the eye gaze of the viewer, and provide an understanding of the interface between digital images and the interpreting pathologist. We aim to study the many variables present in digital platforms, such as the quantity of a sample displayed, and the spacing of tissue profiles, which can create bias in gaze patterns.

Design: Pathologists and trainees were recruited to view a teaching set of whole slide images (WSIs) on a Tobii T-120 eyetracker (120Hz). WSIs were scanned from glass H&E slides, and were viewed using a high performance GPU-assisted client over standard networks. Participants were instructed render diagnoses on a list of WSIs designed to include variation in number and order of tissue profiles. WSIs were modified to alter the number and spacing of profiles within each image, so as to control for any visual bias created by a specific sample. Eye-tracking data including fixation count and duration, as well as time spent within each profile presented were analyzed and compared across sample categories.

Results: Gaze patterns during exploration of WSIs demonstrated that the duration of individual fixations, as well as the visit duration for each profile, were not significantly different between images. As individual fixation and visit durations often correspond to interpretation and complexity of visual processing, this supports the premise that all profiles were of equal visual interest. Visual bias towards specific profiles varied by specimen type, with skin specimens showing a significantly greater number of fixations, as well as time spent, on upper left profiles, regardless of the total number of profiles presented.

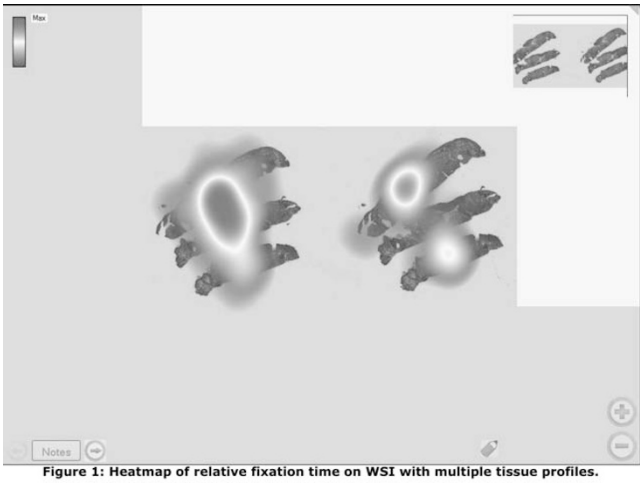

Figure 1: Heatmap of relative fixation time on WSI with multiple tissue profiles.

Conclusions: Initial patterns of gaze suggests biased attention towards specific tissue profiles based upon specimen type, though a dominance of the upper left visual field during initial interpretation of WSIs cannot be excluded. Eye-tracking provides a useful means for quantifying and understanding the optimal presentation of specific specimen types within digital formats.

2136 Interobserver Reproducibility for HER2/Neu Immunohistochemistry: A Comparison of Reproducibility for the Hercep Test™ and the 4B5 Antibody Clone

S Frazier, LJ Layfield, M Esebua, RL Schmidt. University of Missouri, Columbia, MO; University of Utah School of Medicine and ARUP Laboratories, Salt Lake City, UT.

Background: Despite approximately two decades of clinical utilization, HER2/neu testing accuracy remains a major issue for both immunohistochemistry (IHC) and fluorescence in-situ hybridization (FISH) methods. IHC results vary with replicate testing using the same antibody clone and when alternate clones are utilized. IHC results also may be discrepant with FISH. A number of factors appear to be responsible for this variability including fixation times and methods, equipment utilized and training and experience of staff. A number of studies have documented interobserver variability for a single antibody clone but few have evaluated reproducibility between antibody clones and which clones demonstrate the highest degree of interobserver reproducibility and agreement with FISH.

Design: We studied a series of 93 cases stained by both the Hercep Test™ and the 4B5 clone for interobserver reproducibility to determine which clone yielded the best reproducibility and which clone correlated best with FISH. Formalin fixed paraffin embedded sections were stained by the immunohistochemical technique using the manufactures directions in the package insert for both the Hercep Test™ and the 4B5 clone. FISH testing was performed on formalin-fixed paraffin embedded sections according to the PathVysion HER-2 DMA probe kit manufacture's package insert.

Results: Absolute agreement rate for Hercep was 85% whereas the absolute agreement rate for 4B5 was 69%. This difference was statistically significant ($p<0.0001$). The chance-corrected agreement (weighted kappa) for the Hercep Test™ was 79% whereas the chance-corrected agreement for 4B5 was 71% ($p<0.0001$). The absolute agreement rate between antibody clones was 58% with the chance corrected agreement between antibodies being 51%. Absolute agreement of 4B5 with FISH was significantly greater than that of the Hercep Test™ (54% versus 35%).

Conclusions: Agreement between evaluators was greater with the Hercep clone. However, agreement with FISH results was superior for the 4B5 clone. Interobserver agreement was less than the 95% agreement threshold recommended by the ASCO/CAP guidelines for development of a new testing method for HER2 evaluation. This suggests that training programs may be necessary before pathologists should begin evaluation of specimens for HER-2 assessment.

2137 Evaluation of Inflammatory Pathway Mediators in Solid Tumors in FFPE Tissue Using RNAScope

M Gupta, CL Unitt, K Terry, AH Beck. Beth Israel Deaconess Medical Center, Boston, MA; Brigham and Women's Hospital, Boston, MA.

Background: Validation of biomarkers detected through gene expression profiling of solid tumors typically relies on RT-PCR and immunohistochemistry (IHC) both of which have inherent limitations. RT-PCR does not work well on archival formalin fixed paraffin embedded (FFPE) tissues and is unable to separate signals coming from the epithelial, stromal and inflammatory components of the tumor. The application of IHC is also limited by availability of antibodies that work well on FFPE tissue. RNAScope is a recently developed technique that allows in-situ RNA analysis in solid tumors in FFPE tissues. The current study was performed to evaluate TNF-alpha and IL-6 RNA transcripts in a tissue microarray (TMA) of ovarian carcinoma.

Design: A tester tissue microarray including 14 cases of ovarian carcinoma and 16 samples of normal controls was created using acrhival FFPE tissue specimens. Tissue sections, 5μ in thickness, were baked in dry oven at 60°C for 1 hour before performing the RNAScope FFPE assay. Preassay optimization and target hybridization for TNF-alpha (red probe) and IL-6 (green probe) was performed according to ACD RNAscope 2-plex Chromogenic Assay on FFPE tissue. Tonsil tissue was used as a positive control for TNF-alpha and IL-6 RNA transcripts. DapB was used as a negative control. A

positive probe for ubiquitin was used to validate RNA integrity in the analyzed tissues.
Results: High levels of TNF-alpha and IL-6 transcripts were identified in normal tonsillar tissue confirming the validity of the assay. Normal ovarian tissue showed rare single dots for both probes, while 3/14 ovarian carcinomas showed an increased TNF-alpha signals; in 4 cases rare cells with amplified signals were seen; while the remaining 7 tumors were negative. Rare IL-6 signals were seen in three carcinomas.

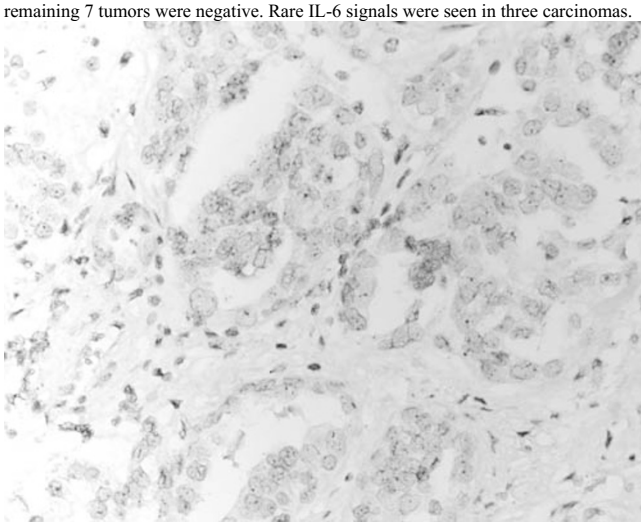

Conclusions: Our findings support the utility of using RNAScope as a novel tool for validating biomarkers detected through gene expression profiling of solid tumors. Inflammatory pathway mediators that cannot be localized precisely to tumor tissue by RT-PCR techniques and lack good antibodies for IHC assays can be easily detected and quantified using this novel technique.

2138 Development and Implementation of an iPhone Application (Pocket Pathologist) to Facilitate Rapid Diagnostic Pathology Consultation

DJ Hartman, SA Yousem, AV Parwani, IC Cucoranu, BJ Kolowitz, W Cable, JS McHugh, GR Lauro, S Sloka, V Palat, AL Von Reden, I Ahmed, L Pantanowitz. University of Pittsburgh Medical Center, Pittsburgh, PA.

Background: Recent technologic advances in eHealth have led to widespread adoption of smartphones to support electronic processes and healthcare communication. Smartphone adaptation for telepathology presents cost savings and efficiency gains. We report our experience with developing an iPhone application (App) to facilitate rapid diagnostic pathology teleconsultation with a smartphone.
Design: A secure web-based portal (https://pathconsult.upmc.com/) was first created to facilitate remote transmission of digital images for teleconsultation. The App augments functionality of the web-based portal and allows the user to quickly and easily upload cases for teleconsultation. Critical to this design was to allow the App to interface with the existing web-based portal. Image quality by the smartphone cameras was evaluated by capturing images using different adapters (Magnifi, Arcturus; SkyLight, SkyLightScope and Snapzoom, HI Resolution Enterprises) that directly attach phones to a microscope ocular lens (Figure 1A).

Results: The App (Figure 1B) facilitated easy submission by limiting the number of data entry fields and uploading images from a smartphone's gallery. The first digital consultation case from China including 18 static images of a pancreatic carcinoma was received 12 days after launch (Figure 1C). Smartphone cameras properly attached to a microscope create static digital images of similar quality to a commercial digital microscope camera at a fraction of the cost and with less complexity.
Conclusions: Smartphones have great potential to support telepathology because they are portable, provide ubiquitous Internet connectivity, contain excellent digital cameras, and can be easily attached to a microscope. Developing an iPhone App, Pocket Pathologist, that allowed users to easily upload digital images via a telepathology web portal allowed our institution to take advantage of these smartphone attributes to facilitate rapid diagnostic pathology teleconsultation, in the absence of expensive stand alone imaging systems.

2139 The Use of Surface Modified Slides in Immunohistochemistry

A Heras, E Oroudjev, A Sanchez, G King. Bio SB Inc, Santa Barbara, CA.

Background: Tissue loss during IHC staining procedures may occur due to weak interaction of a tissue sample with glass surfaces. The present study investigated the surface chemistry of several "hydrophobic" and "hydrophilic" slides and compared the two with regards to tissue retention and reagent dispersal.
Design: Slide reagent dispersal and drop contact angle were measured to assess hydrophobicity and hydrophilicity of slides. X-ray photoelectron spectroscopy was also used to measure the density of amino groups attached to slide surfaces. Slide hydrophilicity was measured depositing 200 µl of dyed tris buffered saline (TBS without detergent) onto the center of each slide. Digital images of slides were captured and analyzed using image analysis software.

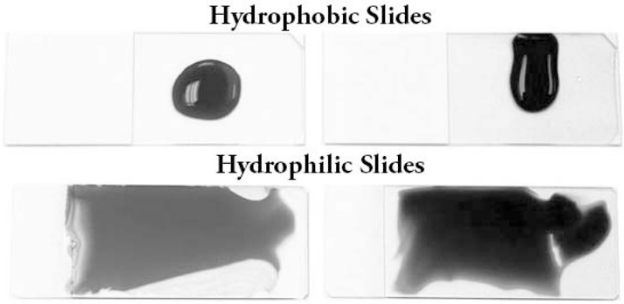

Drop contact angle was measured by depositing 2 µl of TBS on slides and analyzed. 56 FFPE tissues were selected that were known to be prone to detachment after HIER treatment. Tissue adherence was evaluated by measuring the proportion of the total tissue area that remained attached to the slide following HIER treatmen using ImageJ software to calculate tissue retention.The HIER procedure comprised heating deparaffinized sections for 15 min. at 121 C in a pressure cooker with a retrieval solution. Three different pathologists evaluated results independently.
Results: Smaller contact angles on hydrophilic slides indicated greater hydrophilicity and larger contact angles on hydrophobic slides indicated greater hydrophobicity. Hydrophilic slides promoted reagent dispersion and had a much higher tissue retention rate when compared with hydrophobic tissues, with "hydrophobic" slides tissue wrinkling and damage upon retrieval by heat-based methods due to trapping hydrophobic slides trapping water.

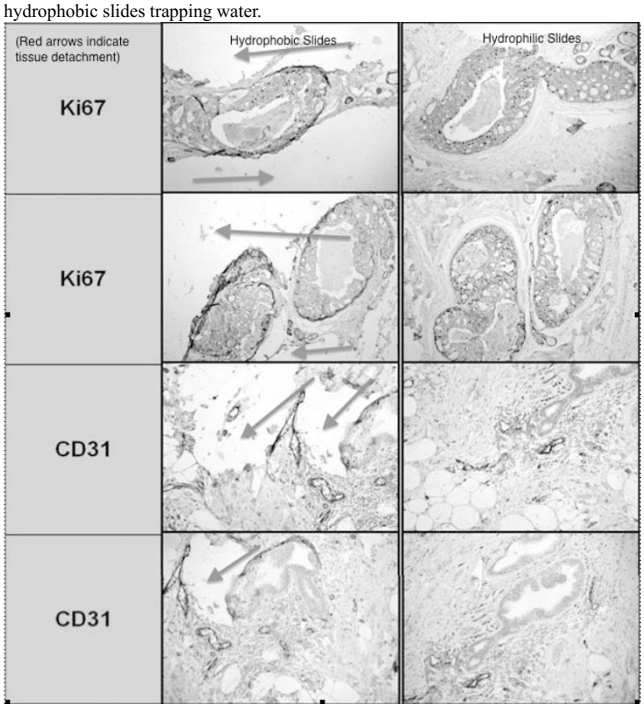

Conclusions: Slides that display more hydrophilic properties than traditional hydrophobic slides are important in preventing tissue detachment and promoting reagent dispersal over the entire working area of the slide to ensure consistent and uniform results in IHC.

2140 New Method for Spatial-Phenotypical Characterization of Cancer-Associated Infiltrating and Stromal Lympocytes

CC Hoyt, C Wang, KL Roman, RL King, MD Feldman. Perkin Elmer, Inc, Hopkinton, MA; Hospital of the University of Pennsylvania, Philadelphia, PA; University of Pennsylvania Health System, Philadelphia, PA.

Background: Successes with PD-L1 drugs and adoptive immunotherapy demonstrate the efficacy of leveraging the immune system to fight cancer. However, host-tumor interaction is complex and difficult to characterize with immunohistochemistry or flow cytometry. Capturing spatial relationships of immune phenotypes in and around tumor is enabled by multiplexed immunofluorescence and multispectral imaging, potentially forming the basis of assays to guide therapy and monitor response. We demonstrate the capability on control and breast cancer samples.
Design: Tonsil and 12 breast cases were labeled for CD4, CD8, CD20, CK, and DAPI, with same-species fluorescence labeling utilizing tyramide signal amplification (TSA). Labels were amplified independently for specific, robust, balanced signals, and analyzed

with the Vectra multispectral automated microscope with pattern recognition software, to segment tumor and stroma and phenotype T and B cells, producing phenotype maps retaining spatial relationships (Figure 1), as varified by a pathologist.

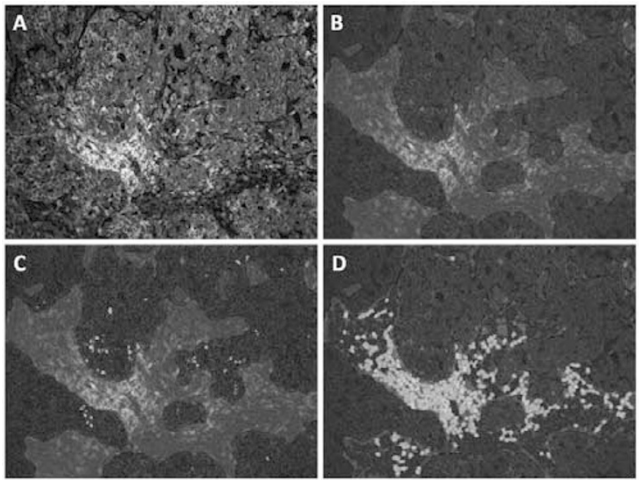

Results: Results demonstrate reliable detection and phenotyping of lymphocytes in heterogeneous clinical samples. Distinguishing inter- and intra-epithelial immune cells was assessed to be > 90% accurate, despite significant inflammation. Tabular data and histogram measures of distance to tumor boundary, both for infiltrating and stromal lymphocytes were created (Figure 2.) Further data will be presented.

	Killer T-cells (CD8+)		Helper T-cells (CD4+)	
Case #	% in tumor	Density (/sq mm)	% in tumor	Density (/sq mm)
#21	8.1%	574	0.9%	67
#22	0.6%	31	0.0%	0
#23	1.7%	99	0.4%	25
#24	6.1%	482	0.0%	10

Conclusions: We believe we have demonstrated a new capability for elucidating the intricacies of cancer immune response, for research and potentially for clinical use, with a workflow that is automated by computer and amenable to present practices where results are reviewed by pathologists to assure data quality.

2141 Immunohistochemical Antibodies Effectiveness in Previously Frozen Tissue

AL Ibarra, ME Vargas. Clinica Las Condes, Santiago, Chile.

Background: Immunohistochemical stains are usually performed on sections of paraffin embedded, formalin fixed material. This methodology is rarely used in previously frozen specimens as intraoperative biopsies. Currently there is no information about the validity of the results obtained in these samples.

Design: Between december 2009 and january 2013, 202 cases were prospectively analyzed with 91 antibodies. The samples more often used were breast, thyroid and soft tissue lesions. Paired tissue fragments, with and without prior freezing in a CO2 microtome, were placed in a single cassette. Immunohistochemical staining was performed in DAKO platform (PT Autostainer Link 48 and Link). Staining protocols used for each antibody were those suggested by the manufacturer. Both authors evaluated immunostained slides independently and in a blinded manner. Those antibodies that proved to be positive on three or more determinations were included in this study.

Results: 64 of 91 antibodies were evaluated on three or more occasions. The average of reactions per case was 14,4 (range from 3 to 93) with a median of 22,26. In 61 of the 64 antibodies (95.3%), the result of the immunostaining was absolutely comparable in samples with and without prior freezing for: cytoplasmic proteins (cytokeratins, vimentin, desmin, SMA, HMB-45, Melan A, synaptophysin, chromogranin, NSE, etc.), surface proteins (CDs, E cadherin) and nuclear proteins (hormone receptors, Ki-67, TTF1, WT1, beta cathenin). Only 3 antibodies results in previously frozen material were poor or erratic (S-100, herceptest and cyclin D1).

Conclusions: In most of the antibodies (95.3%) excellent results were obtained with the immunostaining of paraffin embedded material, previously frozen and formalin fixed. We conclude that, if there are only these kinds of samples, we can trust the results of these determinations almost without exceptions.

2142 Use of Smooth Muscle Myosin Heavy Chain (SMMHC) as an Effective Marker of Follicular Dendritic Cells

I Ioannidis, JA Laurini. University of South Alabama, Mobile, AL.

Background: Smooth muscle myosin heavy chain (SMMHC) is a major structural component of the cytoplasmic contractile apparatus in smooth muscle cells, and therefore, it is considered a relatively specific marker for terminal smooth muscle cell differentiation. Expression of SMMHC in other cell types such as follicular dendritic cells (FDCs) has only rarely been reported. To determine whether SMMHC represents an effective FDC marker in lymphoid tissues, we compared the immunohistochemical results for SMMHC with those of other traditional FDC markers such as CD21 and podoplanin (D2-40).

Design: Sections of 44 formalin-fixed paraffin embedded lymphoid tissues were analyzed, including 31 cases of follicular hyperplasia, 6 cases of follicular lymphoma (FL), 2 cases of peripheral T cell lymphoma , 3 cases of diffuse large B cell lymphoma arising in FL, 1 case of classic Hodgkin lymphoma, nodular sclerosing type, and 1 case of small lymphocytic lymphoma. The overall staining intensity and the extent of SMMHC reactivity within FDCs were compared with CD21 and D2-40. Immunoreactivity was graded semiquantitatively according to the percentage of positive FDCs: 0, <5% FDCs reactive; 1+, 5% to 33.3% FDCs reactive; 2+, >33.3% to 66.6 % FDCs reactive; and 3+, >66.6% FDCs reactive. The intensity of staining was also graded as weak (1+), moderate (2+), or strong (3+).

Results: The sensitivity of SMMHC immunostaining for FDCs was 95.4% and showed no statistically significant difference compared to that of the traditional FDC markers CD21 and D2-40 (97.72 % for both, p>0.05). The extent and intensity of SMMHC positive FDCs were similar to those of D2-40 positive FDCs (Fisher test, p=0.127 and p=0.733 respectively), but significantly lower compared to those of CD21 positive cells (Fisher test, p=0.009 and p=0.00002 respectively). However, in contrast to CD21 which was also positive in some germinal center B cells or to D2-40 which also stained adjacent endothelial cells, SMMHC expression was restricted to FDCs within lymphoid tissues.

Conclusions: Our results indicate that SMMHC is an excellent marker for FDCs, similar to CD21 and D2-40. Moreover, since staining appears to be limited to FDCs in lymphoid tissues, SMMHC can be particularly helpful in demonstrating the underlying architecture in lymphoid processes.

2143 A "Molecular Pap Test" for Cervical Cancer Screening – Detection of HPV Infection and Cellular Abnormalities in Exfoliated Cervical Cells

P Kearney, F Bonnier, C Spillane, F Lyng, C Martin, J O'Leary, S Bakhiet. Trinity College Dublin, Dublin, Ireland; Dublin Institute of Technology, Dublin, Ireland.

Background: The mortality associated with cervical cancer can be reduced if the disease is detected at the early stages of development or at the pre-malignant state. The Pap smear is the current screening method, but is highly subjective and can often exhibit low specificity and sensitivity. For this reason, either a replacement or supportive technique is necessary to improve the quality of cervical cancer screening. Human papillomavirus (HPV) is the main aetiological agent of cervical cancer. Thus, information about the presence and types of HPV in patient samples has high clinical value. Raman spectroscopy is a powerful tool that can generate a biochemical fingerprint of a sample in a rapid and non-destructive manner.

Design: In this study, Raman spectroscopy has been applied to the investigation of cervical cancer cells from PreservCyt specimens. A large library of Raman spectra from HPV positive and negative samples from each cervical intraepithelial neoplasia (Normal, CINI/II/III) grade is being recorded. These spectra will be used to develop an algorithm which can classify unknown spectra based on biochemical changes corresponding to disease onset. In addition, in order to define the specific signature for malignancy, the Raman signal of SiHa cells with a silenced E7 oncogene has been recorded.

Results: Spectral differences exist between superficial, intermediate, and basal cell types in normal cervical cells. Preliminary results also show that Raman spectroscopy is capable of discriminating between normal SiHa cells and SiHa cells containing a silenced E7 gene.

Conclusions: Raman spectroscopy can detect subtle changes between cervical cells, and may be a powerful tool for improved diagnosis of cervical dysplasia.

2144 Human Papillomavirus DNA and Host Gene mRNA Biomarker Detection in a "Micro Total Analysis System" (microTAS) Device to Aid Diagnosis of Cervical Intraepithelial Neoplasia

H Keegan, L Pilkington, R Jordan, J Mozes, N Varga, M Benczik, L Riegger, P Koltay, U Sauer, C Preininger, B Koger, A Brandenburg, W Muller, B Faltin, G Roth, C Martin, C Jeney, JJ O'Leary. Trinity College Dublin and Coombe Women and Infants University Hospital, Dublin, Ireland; GenoID Ltd, Budapest, Hungary; Biofluidix, Freiburg, Germany; Austrian Institute of Technology, Seibersdorf, Austria; Fraunhofer IPM, Freiburg, Germany; Jenoptik Optical Systems GmbH, Jena, Germany; Institut fur Mikrosystemtechnik (IMTEK), Freiburg, Germany.

Background: Human papillomavirus (HPV) DNA detection has high sensitivity for high-grade cervical intraepithelial neoplasia (CIN), but low specificity. Cervical cancer research is focused on development of biomarkers (BM) for prediction of disease severity eg. HPV E6/E7mRNA and p16INK4a/Ki67. This study describes a novel set of host mRNA biomarkers, mediator probe PCR (MP-PCR), and microTAS device for HPV DNA and BM detection in LBC.

Design: A panel of 21 BM were validated by TaqMan PCR assays on 692 women with known histology and HPV status (Hybrid Capture 2 (HC2) and Linear Array HPV Genotyping (LA-HPV)) recruited from colposcopy clinics through CERVIVA (The Irish Cervical Screening Research Consortium) and Jedlik Anyos HPV Screen Multicentric Clinical Study, Hungary. A novel MP-PCR test was designed for HPV and BM detection, clinically validated on AB7900 thermal cycler and miniaturised for use in a microfluidic chip run on an instrument designed for multichannel thermal cycling and fluorophore detection (microTAS device).

Results: Combined BM and HPV testing by TaqMan and hc2 had high specificity (91%), and sensitivity (75%) for CIN1+. HPV16 MP-PCR on AB7900 had high positive predictive value (95%), comparable to HC2 (94%) for CIN2+. On the microTAS device, the HPV16 MP-PCR had a limit of detection of 160 HPV16 copies with high sensitivity (85%) and concordance (82%) to LA-HPV for HPV16 detection. Concordance of TaqMan PCR and the microTAS device for 4 of the mRNA BM ranged from 79% to 83.3%.

Conclusions: Combined mRNA BM and HPV DNA detection by PCR methods may be a useful alternative to consecutive BM and HPV, can be readily adapted for microTAS and should be explored further.

2145 Transcriptome-Wide Biomarker Measurements in Archival Prostate Needle Biopsies for Patient Management

BS Knudsen, LL Lam, N Erho, T Sierocinski, I Tenggara, H Wellman, E Davicioni, J Chan, PR Carroll, HL Kim, MR Cooperberg, JP Simko. Cedars-Sinai Medical Center, Los Angeles, CA; GenomeDx Biosciences Inc, Vancouver, BC, Canada; UCSF, San Francisco, CA.

Background: Enrollment in Active surveillance (AS) programs allows patients to delay and even avoid treatments that carry risk of significant side-effects. Valid molecular biomarkers are needed to identify truly indolent cancers and increase the safety of AS. Challenges with biomarker measurements in biopsies include limited material, tumor and specimen heterogeneity and fragmentation of RNA.

Design: Tissue samples from 23 patients with matched formalin-fixed paraffin-embedded (FFPE) biopsy and radical prostatectomy (RP) specimens were obtained from UCSF and Cedar Sinai. For each patient, samples were taken from tumor, and benign tissue adjacent to tumor (NAT) and from the contralateral side of the prostate (NCT). The tumor content ranged between 5% and 80% of the core length. RNA expression was measured in 130 samples using the 1.4 million feature Affymetrix Human Exon 1.0 ST arrays.

Results: From 1mm cylindrical cores, sufficient RNA was extracted for the assay from 63/69 (91%) biopsy specimens and 69/69 (100%) RP specimens. While the median RNA yield from biopsies was lower than from RP cores, the quantity and quality of c-DNA that was amplified from 100 ng RNA was the same. RNA from 62/63 (98%) biopsies and 68/69 (99%) RP specimens generated expression data that passed quality control. Genomic classifiers (GC) predicting metastasis (GC1) and presence of high Gleason grade (GC2) were highly correlated between matched biopsy and RP specimens with R = 0.74 (p = 0.0003) and R = 0.63 (p = 0.004), respectively. For GC2, matched tumor and NAT from RP had a higher correlation (R = 0.57, p = 0.0045) than matched tumor and NCT (R = 0.10, p = 0.67). There was no relationship between percentage of stromal contamination in the biopsy and the GC scores for either classifier, R = 0.02 (p = 0.91) and R = -0.16 (p = 0.28).

Conclusions: RNA isolated from small amounts of cancer in prostate needle biopsies can be used to measure RNA expression on a genome-wide scale. The data quality is similar to RNA isolated from RP specimens. GC scores from biopsies and RP samples correlate well and are not affected by stromal contamination; and cancer-specific biomarker changes are present in adjacent non-neoplastic tissue.

2146 Validation of a Next Generation Sequencing Biopsy Protocol

M Kossai, M Schiffman, O Elemento, A Sboner, J Fontugne, R Kim, H Beltran, MA Rubin, JM Mosquera. Weill Medical College of Cornell University, New York, NY.

Background: Sampling metastatic tumor sites, especially bone, can be challenging, at times yielding suboptimal tissue even for diagnosis. With introduction of next generation sequencing (NGS) in cancer care, high quality genomic material is required. The following is our multi-disciplinary approach to validate an effective biopsy protocol and tissue processing that generates superior samples for clinical and research application.

Design: This protocol was applied to 15 consecutive biopsies of metastases from patients with advanced prostate cancer, including 5 bone sites. High tumor density areas are identified with PET-MRI and novel interventional radiology tools (i.e. OnControl drill) on a case-by case basis are used. Fresh tissue is transported on wet ice to Pathology. After gross examination, a photograph is taken and tissue is placed on Tissue Tek™ OCT, frozen in isopentane/dry ice combination to avoid freeze artifact. An H&E stained section is reviewed for diagnosis confirmation and evaluation of tumor content. If there are multiple biopsies, each core is embedded separately. After evaluation of all slides, a selected sample is converted to formalin-fixed paraffin embedded tissue for further assays (i.e. IHC, FISH). Slides are annotated to highlight areas for DNA/RNA extraction, then scanned. Real-time updates are provided until pathologic evaluation is finalized. A minimum of 2µg DNA and RNA (RIN> 6) is extracted for sequencing. Corresponding germline DNA from blood is extracted and used to prepare sequencing libraries to cover the whole exome. Sequencing is performed using Illumina HiSeq2500 under rapid run mode (average duration 1.5 days). When amount of tissue is enough, samples are submitted for organoid and xenograft model development.

Results: We had >95% success rate in obtaining high-quality material for NGS using the OnControl drill to biopsy bone sites, 100% success rate for all other sites. The amount of extracted DNA ranged between 200 and 9339.14ng (median 2221.2ng). On average, 99.5% (>170M) and 95.8% (>70M) of paired-end reads generated have been mappable, confirming the high quality of extracted DNA and RNA, respectively.

Conclusions: We have developed a multi-disciplinary approach to validate an effective biopsy protocol that increases the efficiency and quality of metastatic tumor samples for NGS sequencing. The essential role of the pathologist is highlighted. This protocol has been implemented for Precision Care and Clinical Trials at our Institution.

2147 Interobserver Agreement for HER2 Gene Amplification on a New Simultaneous Gene Protein Assay in Breast Cancer

Z Li, A Ranade, D Samrao, J Fine, DJ Dabbs, R Bhargava. Magee-Womens Hospital of UPMC, Pittsburgh, PA.

Background: The combined gene protein assay (GPA) for HER2 (Ventana) is a newly developed technique where both HER2 gene and protein can be simultaneously assessed on a single slide by combining HER2 immunohistochemistry (IHC) with the INFORM HER2 Dual in-situ hybridization DNA probe. The main goal of the study was to evaluate each observer's GPA agreement to fluorescence in situ hybridization (FISH) in HER2 IHC 2+ breast cancer cases.

Design: Tissue sections of 15 invasive breast cancer cases with equivocal HER2 IHC results on clinical testing were included. FISH and GPA were performed on the same tumor blocks. The GPA assay staining results were enumerated by counting at least 20 nuclei by each of the five pathologists blinded to FISH results. For both FISH and GPA, HER2 amplification was defined as HER2/Chr17 or CEP17 ratio 2.0 or higher.

Results: GPA was successful in all 15 cases in the first attempt. All 15 previously tested IHC 2+ cases were again scored as 2+ on GPA. The agreements between FISH and GPA results interpreted by five pathologists (3 in training, 1 with 7 year experience, 1 with 9 year experience) ranged from 93-100% (Table 1).

Table 1: GPA versus FISH for IHC 2+ cases

Observers	Concordant/total cases	Concordance %
1	15/15	100
2	15/15	100
3	14/15	93
4	14/15	93
5	14/15	93

FISH: Fluorescence in-situ hybridization; GPA: Gene protein assay

Two pathologists interpreted one FISH amplified case as not amplified. One pathologist interpreted one FISH not amplified case as amplified. These 2 cases' detailed counts are listed in table 2.

Table 2: Two cases with discordant results

Case #1	HER2 count/cell	CEP17 count/cell	HER2/CEP17 ratio
FISH	5.66	2.91	1.95
OB1	3.40	2.15	1.58
OB2	3.55	2.50	1.42
OB3	5.50	2.35	2.34
OB4	3.45	1.75	1.97
OB5	3.65	2.15	1.70
Case #2	HER2 count/cell	CEP17 count/cell	HER2/CEP17 ratio
FISH	11.07	4.20	2.63
OB1	6.25	2.50	2.50
OB2	7.50	3.40	2.21
OB3	9.95	2.90	3.43
OB4	4.75	3.10	1.53
OB5	4.35	2.75	1.58

OB: observer

The HER2 to CEP17 ratios from all five pathologists and FISH are shown in scatter plot.

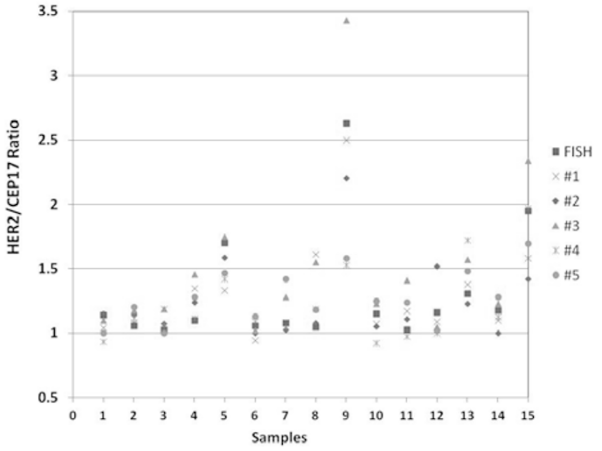

Conclusions: The HER2 GPA shows excellent concordance with both HER2 IHC assay and FISH assay on the most challenging (IHC 2+) breast cancer cases, irrespective of the level of experience of the pathologist. Our study shows high reproducibility of the GPA.

2148 Effects of Slide Storage on PTEN Antigenicity: Implications for Clinical Trials and Translational Research

H Liu, B Mino, E Parra, J Fujimoto, X Tang, A Weissferdt, N Kalhor, II Wistuba, CA Moran, J Rodriguez-Canales. M.D. Anderson Cancer Center, Houston, TX; Xuzhou Medical College, Xuzhou, China.

Background: Phosphatase and tensin homolog (PTEN) is a tumor suppressor gene that regulates cell cycle. Loss of PTEN expression is common in lung cancer, related with increasing in cell proliferation and reduction in cell death. In clinical trials and translational research PTEN expression is analyzed by immunohistochemistry (IHC) on tissue samples including slides stored in pathology archives. However, it is not well known whether PTEN antigenicity is well preserved in stored slides which may account for an incorrect estimation of the actual PTEN expression. Our goal is to study the effect of storage methods for pathology slides on the antigenicity of PTEN.

Design: From the MD Anderson pathology archives 12 cases were selected including 6 cases with surgical resections and 6 cases with cell blocks. All cases were known to express PTEN. The PTEN antibodies used were clones 6H2.1, 138G6, A2b1 and polyclonal. Vimentin was used as indicator of tissue antigenicity. From each case 5 sections were cut; the first section was immediately stained (Time 0), while the rest of the sections were stored for 3 months under the following conditions: 1) room temperature (RT); 2) covered with a seal at RT; 3) cold at 4° C; 4) cold at -20°C. After 3 months the slides were stained in the same way as for Time 0 slides. The slides were scored at the same time using the H-score system.

Results: After storage all PTEN slides suffered loss of antigenicity compared with Time 0. Slides stored at RT showed the greatest loss of antigenicity (27% to 60%). Slides stored at 4°C, -20°C and sealed at RT showed similar loss of antigenicity (up to 30%). Among PTEN clones, 6H2.1 provided the highest expression, but it showed the greatest loss of antigenicity after storage. The polyclonal antibody was less affected by

the storage, but it showed the highest background. A similar trend was observed in the cell blocks, but with more variation of the staining intensity and more background than in the tissue samples. Vimentin expression was not affected after storage.

Conclusions: Our results showed that the storage of slides greatly affects the preservation of PTEN antigen which may result in an underestimation of the actual PTEN expression. The results are variable depending on the clone used. Vimentin expression was not affected, so it cannot predict the tissue antigenicity for PTEN. Our data suggest that PTEN IHC for clinical trials or diagnostic pathology must be performed on fresh cut sections from the block to avoid false negatives, and 6H2.1 might be the best clone.

2149 Optimization of a Cell Transfer Technique for Multiple Immunocytochemistry from Single Cytology Smears for Pathology and Translational Research

B Mino, S Roy-Chowdhuri, I Gonzalez, G Kiriakova, H Liu, J Fujimoto, X Tang, A Weissferdt, N Kalhor, II Wistuba, CA Moran, J Rodriguez-Canales. M.D. Anderson Cancer Center, Houston, TX.

Background: Immunocytochemical (ICC) analysis is an important tool in pathology and translational research. For instance, a large fraction of lung cancer patients are diagnosed on cytology material alone and often times there is no available formalin-fixed paraffin embedded (FFPE) cell blocks or tissues. This is even more relevant in SCLC when the sample is frequently limited and it comprises cytology smears only. In this study, our goal is to optimize a cell transfer technique from cytology smears by transferring tumor cells from a single slide to multiple slides, thus allowing the analysis of multiple biomarkers from limited material.

Design: Cytologic smears of lung cancer cell lines H23 (NSCLC) and H82 (SCLC) were used for technical optimization. Mount-Quick™ mounting medium was used to transfer cells from a single slide to multiple new slides. Parameters tested included type of slide, permeabilization, post-fixation and heat induced antigen retrieval (HIER) techniques. Antibodies tested included keratins, p40, TTF-1, Ki67, Napsin A, chromogranin, synaptophysin, CD56 and MASH1. ICC was tested manually and with an autostainer. We evaluated percentage of transferred cells, cytomorphological quality using an Aperio imaging system and ICC staining before and after cell transfer. The optimazed protocol is then applied on clinical NSCLC and SCLC cases using cytology smears for ICC and compared with that of cell blocks.

Results: The cell transfer was efficient when the original cytology smear was an uncharged slide (95 to 99% of cells transferred vs 15-20% from charged slides). Depending on the cellularity of the cytology smear we obtained between 7 and 20 new slides for ICC. The cell transfer did not affect the cytomorphology or the immunostaining pattern. Our optimized protocol included transferring to coated slides, using HIER and an automated stainer. The application of our optimized protocol on the clinical cases tested so far, including NSCLC and SCLC, provided similar immunoprofile between the transfered cells and the cell block from each case.

Conclusions: The cell transfer technique provided multiple slides from a single cytology smear without altering the cytological features or the immunoprofile. Interestingly, we found that HIER is an important step to improve the efficiency of ICC even for alcohol-fixed cytology smears. In summary, this technique can be applied on clinical cytology smears in cases with limited material for diagnostic ICC or molecular testing even in the absence of FFPE material.

2150 Clinical Validation of Next Generation Sequencing Using Defined Knowledge Resources

C Morrison, L Wei, J Wang. Roswell Park Cancer Institute, Buffalo, NY.

Background: We designed a targeted sequencing NGS assay that includes all all genes for testing in My Cancer Genome. To address the inherent problem of minimizing false positive calls while optimizing sensitivity we used two different NGS methodologies, Ion Torrent and Illumina, as a parallel confirmation of each other.

Design: A parallel system of using the MiSeq and PGM to sequence all specimens within an IT systems control and a "Classify Calls" matrix solution for mutational analysis was designed. Unique cohorts of patients with prior exome sequencing as part of TCGA were used as gold standard controls.

Results: Within the matrix using both the Ion Torrent Suite and MiSeq Reporter platforms we were able to achieve a 99% sensitivity and 100% positive predictive value (PPV). Sensitivity as a single platform was >95% for both PGM and MiSeq, but could not be maximally optimized due to the presence of false positive calls. Using our targeted sequencing panel the PGM consistenly outperformed the MiSeq for the standard performance characteristics of sensitivity and PPV for both frozen and FFPE samples. Both platforms have systematic false positives that are unique and gene specific. As a single platform the MiSeq was plagued by systematic false positive calls that could not readily be removed by quality filters resulting in an optimal PPV of less than 85%. Equally problematic with the MiSeq was systematic errors with high coverage. In comparison false positives in the PGM as a single platform could be removed by quality filters and PPV of 93% could be readily achieved. In addition, systematic errors with the PGM were more limited to variants with lower coverage.

Conclusions: Delivering only the highest quality NGS results to the oncologist for therapeutic decision making requires near perfect sensitivity and PPV. High confidence of the results requires that all variants be confirmed by an independent technology. The Ion Torrent and Illumina technologies are examples of independent technologies and have less in common than does for example Sanger Sequencing with the latter of these two technologies. By designing a matrix solution to parallel sequencing on the PGM and MiSeq we have developed a unique solution to this problem with near perfect sensitivity and positive predictive value that cannot be achieved by either platform alone. Single platform NGS is plagued by false positives.

2151 Utility of Liquid Chromatography Mass Spectrometry (LC-MS) in Identification of Clonal B-Cell Populations

MO Nakashima, C Yuan, S Wang, CV Cotta. Cleveland Clinic, Cleveland, OH.

Background: In research settings liquid chromatography mass spectrometry (LC-MS) is commonly employed for proteomic analysis. LC-MS applications in the clinical laboratory include toxicologic analysis and microorganism identification. Recently this technique has been recognized as the gold standard for identification of amyloidogenic proteins. In spite of this, utilization of LC-MS in surgical pathology is still very limited. When a characteristic immunophenotype is absent, establishing the clonal nature of a B-cell lymphoid proliferation is a crucial step in accurate diagnosis. Flow cytometry, immunohistochemistry and molecular techniques are routinely employed to this end. There are no reliable published studies to date investigating the ability of LC-MS to identify clonal B-cell lymphoid proliferations in formalin-fixed paraffin-embedded tissue (FFPE).

Design: 22 FFPE specimens were analyzed: 7 extranodal marginal zone lymphomas of mucosa-associated lymphoid tissue (MALT lymphomas), 11 amyloidosis cases and 4 benign lymph nodes/tonsils. 5 μm sections were collected on Leica PPS metal frame slides and stained with hematoxylin-eosin. Tissue to be analyzed was visually identified and microdissected on a Leica LMS system, followed by trypsin digestion. Digested products were analyzed on a Thermo Scientific Q Exactive mass spectrometer. Collected data were matched against an IPI human database for protein and peptide identification. Proteins identified were sorted according to peptide spectrum match.

Results: LC-MS analysis of benign specimens showed no evidence of a predominant immunoglobulin. Amyloid specimens showed predominance of lambda light chains in 6 cases, kappa in 3 and transthyretin in 2, as expected, confirming validity of data analysis. MALT lymphoma cases showed a predominant immunoglobulin light chain in 3 of 7 cases; one of these 3 was also diagnosed as light chain deposition disease based on morphology.

Conclusions: LC-MS is not a sensitive method for detection of clonal lymphoid populations in FFPE, even in MALT lymphoma, an entity characterized by abundant cytoplasm and occasional plasmacytoid differentiation. The reason for this is unclear, but we speculate that amounts of intracellular immunoglobulins are relatively small compared to other cellular proteins, cytoskeletal or nuclear, which obscure detection of less abundant proteins. In support of this hypothesis, analysis failed to detect other proteins associated with lymphomas such as BCL-2 or BCL-6. Currently LC-MS is not a useful technique in determining clonality of B-cell populations, even using state-of-the-art instruments.

2152 Liquid Chromatography Mass Spectrometry (LC-MS) Can Identify Post-Translational Modification (PTM) of Histones in Formalin-Fixed Paraffin-Embedded Tissue (FFPET)

MO Nakashima, C Yuan, S Wang, CV Cotta. Cleveland Clinic, Cleveland, OH.

Background: LC-MS is widely employed in research settings for proteomic analysis. Additionally MS is increasingly used in clinical laboratories; MS-based tests are now used to identify drugs/metabolites, microorganisms, and hemoglobin variants. In surgical pathology use of LC-MS is limited to characterization of amyloid, but recent studies have shown that MS analysis of FFPET can yield results similar to those obtained from fresh tissue opening the possibility of performing proteomic analysis on archived tissue, potentially leading to discovery of new markers and therapeutic targets. Many proteins undergo significant PTM; most biological processes are controlled to some extent by PTM such as phosphorylation, acetylation, methylation, and ubiquitination. Drugs targeting kinases, deacetylases, and methylases are currently employed to interfere with PTM and alter viability of neoplastic cells. Identification of drug targets and monitoring target effects is difficult in-vivo. LC-MS can identify common PTM in cell cultures and fresh samples. To our knowledge there are no studies investigating use of LC-MS to identify PTM status of proteins in FFPET. To fill this void, we attempted to use LC-MS to detect methylated histones in FFPET.

Design: 7 FFPET blocks were selected, representing a range of tissues (2 benign colon, 3 colon carcinoma, 2 tonsil). Sections were collected on Leica PPS slides and H&E stained. A Leica LMS system was used to microdissect approximately 100,000 nm^2 of tissue, which was digested with trypsin, then analyzed on a Thermo Scientific Q Exactive mass spectrometer. Results were matched against the IPI human protein database. Further analysis was performed to identify histone peptide fragments which had been methylated.

Results: Histone (H)2A was the most common histone, detected in 7/7 samples. All showed methylation (M) at K119 and K120, while in 3 K96(M) was also present. In 5/7 we identified H4, all with K80(M) and 3 also with K32(M). H3K80(M) was present in 5/7; 2 also with H3K100(M). H1K35(M) and H1K47(M) were seen in 3/7, while H2BK109(M) was detected in only 1.

Conclusions: Use of LC-MS in FFPET is still limited as the impact of formalin-fixation on the ability of LC-MS to identify proteins is not fully investigated. We show that LC-MS can identify specific proteins (histones) in FFPET as well as their PTM status despite relatively harsh preparation protocols. Gentler preparation and more elaborate data analysis are likely to significantly increase assay reliability and allow identification of a wider spectrum of PTM.

2153 Comparison of Aldehyde and Alcohol Fixatives in Preservation of Low and High Copy Number Genes

M Nassiri, M Nadji, A Morales. Indiana University School of Medicine, Indianapolis, IN; University of Miami Miller School of Medicine, Miami, FL.

Background: Tissue-based molecular studies are becoming important part of clinical diagnostics. However, in contrast to body fluid-based methods where quality control standards are well defined, there are no well defined pre-analytical standards for tissue-

based molecular studies. The purpose of this study was to evaluate the effect of various tissue fixatives, before and after processing, on the quality of transcript preservation of low and high abundance genes.
Design: Mouse liver tissue was dissected into small cubes of 0.5x0.5x0.2 cm, weighing ~100 mg, and immediately immersed in 50 ml of the following fixatives: aldehyde based -10% neutral phosphate buffered formalin (4% formaldehyde), Mirsky, Notox, Prefer, Preserve, Streck, Glycofix, Omnifix; and alcohol based-70% ethanol, Methacarn, Statfix, F13, Krayofix, Statfix, and Molecular Fixative . The exposure times for all fixatives were 1 hour and 24 hours at room temperature. RNA was isolated from each sample following the exposure periods by the Trizol method. Duplicate sets of each sample were also processed immediately after fixation periods by a formalin-free microwave-based tissue processor (Tissue-Tek® Xpress™, Sakura Finetek, Torrance, CA). RNA was extracted from paraffin embedded tissue using Ambion FFPE kit. RNA isolated from similar volume and weight of fresh mouse liver tissue served as positive control. All samples were run in triplicate and each experiment was repeated at least twice. Quantitative real-time PCR for a high (GAPDH) and a low (FOLH, Folate hydrolase 1) transcript copy number genes was performed using cDNA synthesized from 10ug total RNA using Invitrogen (Carlsbad, CA) Cloned AMV cDNA synthesis kit and random hexamers.
Results: Alcohol-based fixatives consistently showed higher yield of RNA and less degradation when compared to aldehyde-based fixatives. There was a considerable decline in the quality of RNA and a decrease in transcript copy numbers with longer exposure time to aldehyde fixatives but not to alcohol fixatives. Both low and high copy number genes were detected in alcohol fixatives in contrast to aldehyde fixatives.
Conclusions: Alcohol-based fixatives are more reliable than aldehyde-based fixatives for preservation of gene transcripts. The superiority of alcohol fixatives in preservation of nucleic acids is also maintained following the processing of tissue using a formalin-free processing platform.

2154 Enhancement of Loop-Mediated Isothermal Amplification for Detection of African Trypanosimes in Cerebrospinal Fluid in Clinnically-Defined Samples

OV Nikolskaia, S Bisser, B Courtioux, JS Dumler, DJ Grab. The Johns Hopkins University School of Medicine, Baltimore, MD; Université de Limoges, Institut de Neurologie Tropicale, Limoge, France.
Background: In rural Africa, failure to microscopically diagnose infections by *Trypanosoma brucei gambiense* (*Tbg*) or *T. b. rhodesiense* (*Tbr)* in blood smears and/or CSF in the critical early stages of the disease is the single most important factor in failed treatment.The loop-mediated isothermal amplification (LAMP) assay has evolved as one of the most sensitive and specific methods for the detection of a broad range of pathogenic microorganisms including African trypanosomes.
Design: Using LAMP assays targeting multicopy gene targets, we previously showed that by simply adding detergent into control non-HAT blood or cerebrospinal fluid spiked with trypanosomes during sample preparation, that clinical sensitivities for LAMP that mimic analytical limits could be approached or even be obtained. We assessed the ability of detergent-enhanced LAMP assays to detect trypanosomes in clinically defined samples. We used a defined cohort of 183 CSF samples obtained from HAT patients in Angola, Central African Republic, Democratic Republic of Congo and Gabon. For controls, we tested CSF from 100 de-identified non-HAT patients. One uL 10% (w/v) Triton X-100 was added to 19 uL CSF and allowed to stand at ambient temperature for 60 min before use in LAMP assay. Statistical significance was determined using 2-sample paired Student's t-test. Based on a 1 uL sample size, the detection limit for LAMP was thus set at ~50 parasites/mL.
Results: While none of the control CSF samples from non-HAT patients were positive for parasite DNA, remarkably trypanosome DNA was detected at the same frequency in type 1 and 2 HAT patients. Without detergent only 2% of the samples were positive for parasites. However, the addition of detergent to the samples prior to assay increased overall assay sensitivity >15 fold. Our results were confirmed using LAMP primers targeting a putative *Tbg*-specific C_3A tetra-nucleotide sequence in the multi-copy *Tbg* 5.8S rRNA-internal transcribed spacer 2 (5.8S-ITS2) gene (Genebank Accession No. AF306777).
Conclusions: Recent studies in murine models have shown that African trypanosomes have the potential to enter the CNS soon after entry into the bloodstream. Whether the detection of parasites in Stage 1 CSF provides supportive clinical evidence for early CNS entry or simply reflects contamination by parasite-infected blood during lumbar puncture are important considerations for future studies.

2155 Temperature Calibration of Well-to-Well Variation during High-Resolution Melt Analysis by Novel Unlabeled Stem-Loop Oligonucleotides

RH Nussenzveig, HT Pham, E Lyon, ME Salama, C Wittwer, AM Agarwal. University of Utah and ARUP Laboratories, Salt Lake City, UT.
Background: Single, closed-tube genotyping of small amplicons by HRM using DNA intercalating fluorescent dyes is a rapid, low-cost alternative to methods such as pyrosequencing or use of labeled oligonucleotide probes. Yet, variables such as DNA extraction method and concentration lead to within run sample melt discrepancies. Moreover, homozygous base-pair neutral single nucleotide polymorphisms (SNP), in particular those in classes 3 and 4, can be difficult to genotype accurately due to small differences in melt temperature (T_m). Use of two complementary oligonucleotides as melt calibrators has proven useful for discrimination of temperature shift neutral polymorphisms and for DNA samples from different sources (*eg.* fresh tissue and FFPE), purified by different procedures, or at different concentrations. Current technology requires the use of 3'end blocked, PAGE purified complementary oligonucleotides (total of 4) for low and high T_m calibration. The cost of each blocked and purified oligonucleotide is high, and yield is generally less than 5% after purification.
Design: In order to overcome these challenges we developed a novel type of melt temperature calibrator based on formation of a blunt-end stem loop structure and a single oligonucleotide probe.
Results: Hairpin melt calibrators of both low and high T_m have been developed. Annealing and melt of complementary oligonucleotides follows the physical principles of Brownian motion and random collision making such events dependent on oligonucleotide concentration and complexity of the environment. In contrast, such limitations do not affect our novel calibrator design since complementary sequences within the stem structure are always close by and their annealing thus follows a 0^{th} order reaction. Both hairpin calibrators were compared experimentally with complementary oligonucleotide calibrators (Idaho Technology, Salt Lake City, UT). Different temperature shift neutral SNPs were selected for comparison. Our results indicate melt temperature calibration using our novel stem loop calibrators perform as well as complementary oligonucleotide calibrators.
Conclusions: The low cost for synthesis and concentration independence facilitate robust signal detection across platforms and make it very useful in the clinical laboratory setting.

2156 Comparison of Automated Immunoassay and Liquid Chromatography Tandem Mass Spectrometry for 25-Hydroxyvitamin D

S Parajuli, S Bhattacharyya, N Hotchandani, A Khan, BM Goldsmith. Temple University Hospital, Philadelphia, PA; Temple University School of Medicine, Philadelphia, PA.
Background: Vitamin D deficiency and/or insufficiency resulting in various skeletal and extra-skeletal morbidities have increased clinical interest in vitamin D worldwide. 25-Hydroxyvitamin D [25(OH)D] is the major circulating and storage form of vitamin D and is considered the best marker for screening vitamin D status. The reference method for measuring 25(OH)D is Liquid Chromatography Tandem Mass Spectrometry (LCMS/MS) in serum or plasma, often performed by reference laboratories. LCMS/MS quantitates ergocalciferol (D2) and cholecalciferol (D3) forms of vitamin D. Immunoassays have been developed for total 25(OH)D where D2 and D3 are not separately measured. These assays can be performed on routine clinical laboratory analyzers, reducing the turnaround time and decreasing send-out costs.
Design: We compared the LCMS/MS method (Quest Diagnostics) with immunoassay on the Abbott Architect i2000 SR (Abbott Diagnostics). Specimens were analyzed by both methods. Patient demographics, clinical information, and vitamin D and /or calcium supplementation was obtained where possible. EP Evaluator was used to determine precision and correlation data (Data Innovations).
Results: The immunoassay method was linear between 3.8-75 ng/mL. Intra-assay precision (%CV) (Low, Medium, High Controls, Abbott Laboratories) was 3.3%, 3.1% and 2.3% for levels low, medium and high respectively. Inter-assay precision (%CV) was 7.7%, 4.2% and 3.9% for levels low, medium and high respectively. The Correlation Coefficient (r) for all specimen was 0.6946 (n=130, slope=0.67, y-intercept 5.01). For results <30 ng/mL by LCMS/MS (reference range), r=0.7398 (n=82, slope 1.089, y-intercept -2.36). Patients were further classified into the following groups for statistical analysis: Gender, Age (increments of 10 years), Ethnicity (Caucasian, Hispanic, Non-Hispanic), Supplementation (Vitamin D, Calcium, Both), and patients with renal disease. Correlation data for each group ranged from r=0.2977 to r=0.9929. We found that in 13% (n=17) of specimens, D2 measured by LCMS/MS was higher than total 25(OH)D measured by immunoassay.
Conclusions: Our results show that the Architect immunoassay for total 25(OH)D was acceptable as a screening method for levels <30 ng/mL and can be used as an alternative to LCMS/MS. Caution in the interpretation of results should be taken as an increase in D2 may decrease the total 25(OH)D level by immunoassay. This occurs only when patients are taking D2 supplements.

2157 Preserving High RNA Quality during Laser Capture Microdissection of Frozen Tissue Sections

K Pereira, J Jiang, L Ailles, MHA Roehrl. Princess Margaret Cancer Center, Toronto, ON, Canada; University Health Network, Toronto, ON, Canada.
Background: Laser-capture microdissection (LCM) is one of the best techniques for isolating pure populations of cells for downstream molecular analyses of DNA or RNA. One of the most important issues is to reliably distinguish the cells of interest. Preserving good tissue morphology can often be difficult when using frozen sections and should not come at the expense of RNA quality. Thus, a balance between the two must be found. In this study, we isolated tumor and tumor stromal cells from frozen sections of head and neck squamous cell carcinoma (HNSCC) samples for the purpose of extracting RNA to be used downstream in gene expression microarrays. Here, we describe the optimization of our method.
Design: Frozen tissue sections were cut, placed on membrane slides, fixed, and stained with a light hematoxylin (1:10 dilution) stain. Standard hematoxylin and eosin staining cannot be used since it has been shown to degrade RNA. LCM (Leica) method optimization was performed on 4 pilot patients generating 8 samples (4 cancer and 4 tumor-associated stroma), each containing 20-50 thousand cells. The optimized protocol was validated on 16 samples (8 cancer and 8 tumor-associated stroma) from 8 patients.
Results: Diluted hematoxylin was able to provide the contrast necessary to distinguish tumor from stromal cells while maintaining RNA quality. Following staining, we tested the RNA stabilization effect of keeping the slides at -80°C versus keeping them at room temperature prior to starting LCM. We found that keeping the slides at room temperature after staining did not affect RNA quality but yielded better histomorphology for LCM microdissection. The effect of collecting captured cells directly into lysis buffer (Qiagen RNeasy Micro Plus kit) compared to collecting into RNA Later solution (Ambion) was also tested. We found that cells collected in RNA Later yielded better quality RNA compared to tissue collected in lysis buffer (mean RIN score of 8.1 vs. 4.6). Using the

optimized protocol on 8 HNSCC patients yielded mean (±SD) RIN scores of 7.5±0.6 for tumor and 6.5±0.4 for tumor stroma, respectively. Average corresponding extractable RNA concentrations were 13.6 and 8.9 ng/μl, respectively.
Conclusions: When performing LCM on frozen tissue sections, our study indicates that using a dilute hematoxylin stain on the tissue, keeping LCM membrane slides at room temperature post-fixation, and collecting the captured tissue in RNA Later solution yields RNA of consistently high quality for downstream microarray gene expression studies.

2158 Using Primary Tumor Cells from Patients to Investigate the Early Steps of Metastatic Dissemination

J Pignatelli, S Goswami, X Chen, E Adler, J Jones, J Condeelis, MH Oktay. Albert Einstein College of Medicine, Bronx, NY; Montefiore Medical Center, Bronx, NY.
Background: Cell lines are widely used as *in vitro* models to study cancer cell biology. Despite numerous advantages there is growing evidence that cell lines do not faithfully represent tumor cells *in vivo* due to intra- and inter-laboratory cell line heterogeneity and drift away from the phenotype of the original tumor due to immortalization and time in culture. This is a serious concern especially if cell lines are assumed to be valid models for evaluating the pathobiology of breast cancer and/ or the likely response to novel targeted therapies. We have developed a novel approach to study the initial step of metastatic dissemination, transendothelial migration (TEM), *in vitro* using primary breast cancer cells from patients.
Design: We obtained breast cancer cells from 25 surgical resections of invasive ductal carcinomas of the breast by fine needle aspiration (FNA) using 25 gauge needle and developed conditions suitable for short term *in vitro* survival and intravital labeling of these cells. We assessed their TEM activity using subluminal-to-luminal transwell assay engineered with human umbilical vein endothelial cells (HUVEC) and visualized TEM by confocal microscopy.

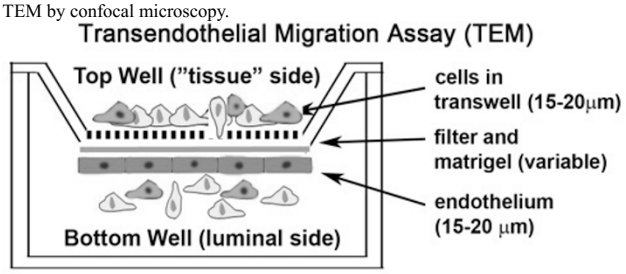

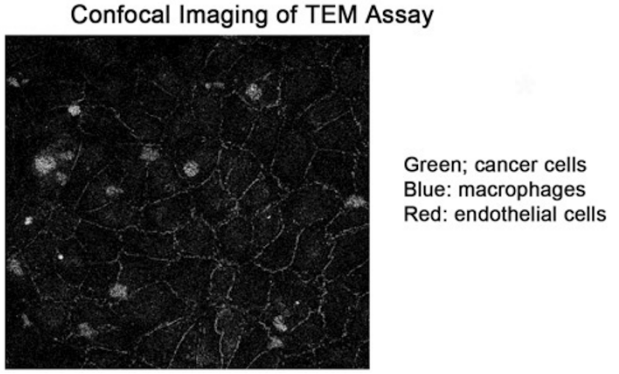

Actin regulatory protein Mena isoform expression pattern known to be associated with disseminating tumor cells *in vivo* ($Mena^{INV}$ high – Mena11a low) was used to confirm the presence of TEM-competent cells on the luminal side of the assay.
Results: From all 25 cases, using FNA we obtained a 90-95% pure cancer cell population containing viable cells suitable for labeling with intravital tracker dyes. Cancer cells from three major clinical subtypes; $ERPR^{+}/Her2^{-}$, triple negative and $Her2^{+}$ were capable of TEM *in vitro*. In all cases but one, TEM competent cells showed *in vivo* Mena isoform expression pattern, $Mena^{INV}$ high – Mena11a low. By comparison, cancer cell lines such as MDA-MB 231 did not consistently demonstrate either TEM or the *in vivo* Mena splice variant expression pattern.
Conclusions: Cancer cells obtained from patient breast cancers by FNA can be successfully used *in vitro* to study TEM and potentially to assess the effect of novel drugs that target cancer cell TEM and therby intravasation.

2159 Interphase and Mitotic Cells in High-Grade Clinical Cancers Display Robust Centrosome Amplification and Clustering Compared to Cells Cultured *In Vitro*

MD Reid, V Pannu, B Celik, PCG Rida, R Aneja. Emory University School of Medicine, Atlanta, GA; Georgia State University, Atlanta, GA.
Background: Centrosome amplification (CA) is a hallmark of cancers. In cells with supernumerary centrosomes, centrosome clustering during mitosis facilitates evasion of the catastrophic consequences of a multipolar mitosis and allows perpetuation of chromosomal instability via low-level chromosomal missegregation. In this study, we analyzed the frequency of CA and the spatial distribution of supernumerary centrosomes in interphase and mitotic cells within several clinical tumor types and compared them with similar type tumor cells cultured *in vitro*.
Design: Centrosomes and microtubules were visualized by immunostaining for γ-tubulin (green) and α-tubulin (red), respectively. DNA was stained with DAPI (blue). We evaluated colonic (n=12), cervical (n=13), bladder (n=33), breast (n=50) and pancreatic (n=45) carcinoma for frequency of CA and organization of amplified centrosomes in both interphase and mitosis. Percentages were calculated from 10 random fields in each sample. In comparison, we evaluated various cancer cell lines including HT-29 (colon), HeLa (cervix), T24 (bladder), MDA-MB-231 (breast) and MiaPaCa (pancreas) for CA status in random cell populations and counted 1000 tumor cells in each case.
Results: Centrosome amplification ranged from 60-85% cells in all clinical tumor types ($p<0.001$). Interestingly, the majority of amplified centrosomes in tumors were clustered both in interphase (~90%) and mitotic (80-90%) cells. By comparison, in cultured cell lines we found that only 5-20% of cells exhibited amplified centrosomes ($p<0.001$), indicating that cell lines had significantly lower frequencies of CA than those observed in patient tumors. Multiple centrosomes occurred either as a cluster in interphase cells (~80%) or as two clusters at the two poles of pseudobipolar mitotic spindles (60-80%).

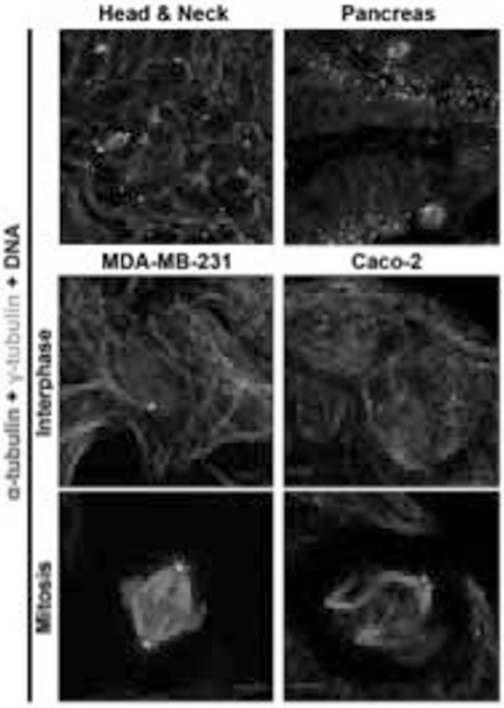

Conclusions: Unlike cultured cells, an overwhelming majority of patient tumor cells in high-grade cancers are in interphase and bear aberrant, amplified centrosomes that are commonly segregated into daughter cells as two clusters via pseudobipolar mitoses. These supernumerary centrosomes remain "huddled" together in a clustered configuration through interphase.

2160 Centrosome Amplification: A Quantifiable Cell Biological Trait

MD Reid, R Paranjpe, S Dharma, B Celik, V Pannu, J Gaitor, N Wright, P Patel, M Hoque, PCG Rida, R Aneja. Emory University School of Medicine, Atlanta, GA; Georgia State Univerisity, Atlanta, GA.
Background: Cancer cells frequently exhibit numeric and structural centrosomal aberrations, termed centrosome amplification (CA). However, a method of quantifying CA in various tumors is lacking. We pioneered a simple method to quantitate the degree of CA (both numeric and structural) within multiple tumor samples.
Design: We performed a quantitative comparison of centrosomal aberrations in grade-matched breast, bladder and pancreatic carcinomas. Tissue Microarrays (TMAs) from grade-matched biopsies/resections of breast (n=35), bladder (n=33) and pancreatic (n=20) carcinomas were immunostained for centrosomes, and co-stained with DAPI nuclear stain. Immunofluorescence confocal imaging was then used to stack optical sections of tumor tissue and capture all centrosomes and nuclei within 15 regions of interest (ROIs) per sample. Centrosomes were categorized as (i) individually-distinguishable centrosomes (iCTRS) or (ii) as megacentrosomes (mCTRs) comprised of several tightly clustered centrosomes whose precise number could not be determined. For each ROI, the number of nuclei as well as the numbers and volumes of all iCTRs and mCTRs were determined. A cumulative Centrosome Amplification Score (CAS) was obtained for each ROI using the following formula:

$$CAS = \frac{\text{No. of iCTRs}}{\text{No. of nuclei}} + \frac{\text{No. of mCTRs}}{\text{No. of nuclei}} + \frac{\text{Avg. vol. of iCTR}}{\text{Avg. vol. of normal CTR}} + \frac{\text{Avg. vol. of mCTR}}{\text{Avg. vol. of normal CTR}}$$

Results: Nonneoplastic tissue did not exhibit CA, and had CAS values well within the predicted range of 2-3. In contrast, the average CAS values for tumors were significantly higher, with breast tumors exhibiting higher CAS values (CAS range 4-47) than bladder (CAS 5-18) and pancreatic cancers (CAS 5-16). All tumors (n=88) exhibited significantly higher CAS values than their adjacent nonneoplastic counterpart ($p<0.01$).
Conclusions: Quantification of CAS in tumor samples establishes CA as a "quantifiable cell biological property" that enables us to quantitatively determine the extent and severity of numeric as well as structural centrosomal aberrations.

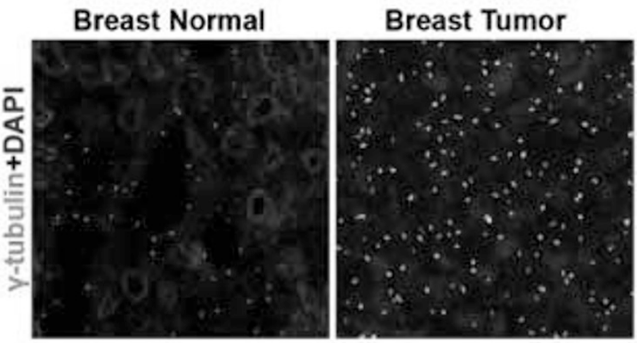

2161 Downfall of the 'Mitotic Monarchy': A Comparative Analysis of Mitotic Indices in Patients' Tumors Versus Those in Cancer Cells Cultured *In Vitro*

MD Reid, V Pannu, PCG Rida, R Aneja. Emory University School of Medicine, Atlanta, GA; Georgia State University, Atlanta, GA.

Background: Mitosis-targeting drugs under clinical development have failed to translate their preclinical efficacy into clinical response in human trials. Their clinical failure has challenged the prevalent notion that cells in patients' tumors divide frequently, similar to cancer cells observed in *in vitro* cultures and in xenograft models. We investigated the concordance between clinical tumor samples and *in vitro* cultured cells by evaluating the degree of mitotic activity.

Design: Centrosomes and mitotic spindles were immunostained using anti-γ-tubulin and anti-α-tubulin antibodies, respectively, and visualized using indirect immunofluorescence confocal imaging of paraffin-embedded clinical cancer samples derived from high-grade carcinomas of the colon (n=12), cervix (n=13), bladder (n=33), breast (n=50) and pancreas (n=45). For comparison, we also determined the same parameters in matched adjacent non-neoplastic tissue. The percentage of mitotic cells were quantitated from 10 randomly selected fields per sample (at least 500 cells were counted per sample). We similarly screened various cancer cell lines including HT-29 (colon), HeLa (cervix), T24 (bladder), MDA-MB-231 (breast) and MiaPaCa (pancreas) for mitotic cells by counting 1000 cells from random cell populations.

Results: We found that <2% of cells ($p<0.001$) were in mitotic phase in all clinical tumor types. Surprisingly however, in the cancer cells that were cultured *in vitro*, the population of cells in mitotic phase ranged from 4-18% ($p<0.001$), with the highest proportion present in human breast MDA-MB-231 cell lines.

Conclusions: This is the first report comparing mitotic indices in highly mitotically active *in vitro* cell cultures with the cancer cells in patients' bodies, and it showed that mitotic indices were strikingly lower in the latter group, compared to cell lines.. The low indices observed in patients' tumors validate the notion that mitosis is a poor therapeutic target, and emphasizes the need to explore the development of agents that target interphase processes, specifically in patients' cancer cells.

2162 Development of an In Vitro Model of Germinal Center Lymphomagenesis

CL Robinson, RM Paolino, TA Summers, DJ Hodson, LM Staudt. WRNMMC, Bethesda, MD; NCI/NIH, Bethesda, MD.

Background: Next generation sequencing of germinal center derived malignancies such as DLBCL and Burkitt lymphoma has generated a myriad of recurrently mutated genes. While the oncogenic effect of some of these mutations is understood, the functional consequence and synergistic interaction of most remain largely uninvestigated. Elucidating the effects of these mutations may reveal which are key drivers of lymphomagenesis and aid in the development of new, targeted therapies. Current methodologies include genetically modified mice and lymphoma cell lines. Mouse models are impractical for testing multiple combinations of mutations. Lymphoma cell lines are typically characterized by complex genetic changes and are derived from late stages of disseminated malignancy. As such, neither is ideal to study the early stages of lymphomagenesis. We are developing an *in vitro* cell culture system that involves the genetic modification of non-malignant, human, primary germinal center B-cells to investigate the effect of individual oncogenic mutations and synergy between combinations.

Design: Tonsil-derived, human, primary germinal center B-cells were cultured with fibroblasts expressing CD40 ligand. The B-cells were then infected with one or more retroviruses, each expressing an oncogene of interest along with a different stainable cell-surface marker. This allows the relative proportions of cells expressing single or multiple oncogenes to be assessed over time by flow cytometry.

Results: To confirm the ability of the system to demonstrate synergy between oncogenes, we used the well-established oncogenic combination of BCL2 and MYC. The clear expansion of doubly transduced cells over a 10 day period showed the synergistic effect. Double positive cells represented less than 10% of the cells at day 2, and were more than 90% of the culture by day 12. Shortly after this time point, cells both transduced and non-transduced ceased their previously vigorous proliferation, seemingly due to the terminal differentiation of the cells.

Conclusions: We have demonstrated a viable proof of concept to model the genetics of lymphomagenesis that is not subject to difficulties associated with cell lines or murine models. The limited lifespan of infected cells to date has thus far restricted the ability to investigate the function of weaker oncogenes in lymphomagenesis. Modifications to cell culture conditions and the oncogenes transduced may allow us to circumvent this problem in the future. Overall, this approach to modelling the genetics of lymphomagenesis appears promising and may potentially aid in the development of novel therapies.

2163 Targeted Next Generation Sequencing of Adenocarcinoma of Unknown Primary Site Reveals Frequent Actionable Genomic Abnormalities and New Routes to Targeted Therapies

JS Ross, K Wang, GA Otto, G Palmer, R Yelensky, D Lipson, J Chmielecki, SM Ali, D Morosini, VA Miller, PJ Stephens. Albany Medical College, Albany, NY; Foundation Medicine Inc, Cambridge, MA.

Background: Metastatic adenocarcinoma of unknown primary site (ACUP) has a poor prognosis with currently utilized non-targeted systemic therapies achieving only modest success at preventing disease progression. In this study, a comprehensive genomic profiling assay was evaluated for its ability to identify potential targets of therapy for ACUP patients not currently tested for in routine practice.

Design: Hybridization capture of 3,769 exons from 236 cancer-related genes and 47 introns of 19 genes commonly rearranged in cancer was applied to≥ 50ng of DNA extracted from 127 ACUP FFPE tumor specimens and sequenced to high, uniform coverage. Genomic alterations (base substitutions, small indels, rearrangements and copy number alterations) were determined and then reported for these patient samples. Actionable GA were defined as those identifying anti-cancer drugs on the market or in registered clinical trials.

Results: There were 74 female and 53 male ACUP patients with a median age 57.2 years (range 25-85 years). Most common sample sites were liver (24%), lymph node (23%), peritoneum (16%), pleura (6%), bone (5%) and brain (4%). IHC workup was performed on 93% and mRNA profiling on 3% of ACUP cases. A total of 484 alterations were identified, 3.8 GA per tumor (range 1-10), with 115/127 (91%) ACUP cases harboring at least one actionable GA . The GA included 260 base substitutions, 63 indels, 100 gene amplifications, 47 gene homozygous deletions and 14 gene rearrangements. Of 116 genes with GA, 51 (44%) were actionable. Of 58 genes altered in more than 1 tumor, 30 (51%) were actionable. The most common actionable alterations were mutation, amplification homozygous deletion or fusion of *KRAS* (23%), *CDKN2A* (23%), *MCL1* (11%), *NF1* (9%), *ERBB2* (9%), *PTEN* (8%), *PIK3CA* (7%), *EGFR* (7%), and *BRAF* (6%). Eighty-seven (69%) of ACUP had at least one actionable GA in the RTK/RAS signaling pathway including *EGFR*, *FGFR1*, *FGFR2*, *KRAS*, *NRAS*, *BRAF*, *MAP2K1*, *NF1*, *NF2*, *ARAF*, *RAF1*, *MET*, *RET*, *ROS1*, *KIT*, and *ALK*. RTK/RAS pathway GA were mutually exclusive.

Conclusions: More than 90% of the ACUP patients in this study harbored at least one actionable GA with the potential to influence and personalize therapy selection. Given the limited treatment options and poor prognosis of patients with ACUP, comprehensive NGS-based genomic profiling has the potential to identify new treatment paradigms and meet an unmet clinical need for this disease.

2164 High Variability in Sensitivity and Specificity of MET IHC Antibodies Presents a Challenge for the Identification of Patients for MET-Targeted Therapy

S Rost, C Lowe, H Koeppen. Genentech, South San Francisco, CA.

Background: MET-targeted therapy has shown clinical promise in two clinical studies, rilotumumab (anti-Hepatocyte Growth Factor antibody) in gastric cancer and onartuzumab (anti-MET antibody) in non-small cell lung cancer (NSCLC). In the NSCLC trial patient tumors were classified as MET-positive or MET-negative by immunohistochemistry (IHC) using the SP44 anti-MET rabbit monoclonal antibody (Ventana). Onartuzumab in combination with erlotinib showed improved survival in MET-positive patients but worse clinical outcome in MET-negative patients. This observation highlights the importance of a robust, validated IHC assay to determine MET status of tumors in patients considered for MET-targeted therapy. In this study we evaluated the performance of 9 MET IHC antibodies (Table 1) using a variety of staining conditions and compared it to our clinically validated SP44 MET IHC assay.

List of MET antibodies

Vendor	clone or product #	Isotype*
Ventana Inc. & Spring Bioscience	SP44	rb IgG
Cell Signaling	D1C2	rb IgG
My Biosource	3D4	ms IgG2a
IBL	polyclonal #18321	rb IgG
Santa Cruz	N-17; C-12; C-28	gt IgG; rb IgG; rb IgG
Abcam	8F11	ms IgM
R&D Systems	polyclonal #AF276	gt IgG

* rb:rabbit, ms:mouse, gt:goat

Design: IHC was performed on paraffin sections of a two tissue microarrays representing eight cell lines with defined (by IHC, Western blot and RNA levels) MET expression and NSCLC tissues of known Met status, respectively. Antibodies were tested on the Ventana Benchmark XT, Leica BOND-III, Dako Autostainer Plus and Dako Omnis using 14 different AR and detection methodologies.

Results: The only antibodies with sensitive and specific staining equivalent to the clinically validated assay were SP44 and D1C2 when used under the following conditions: Ventana Benchmark XT with CC1 standard, CC1 extended and CC2 AR; -Leica BOND-III with ER2 AR; DAKO Autostainer Plus with low pH AR and Envision-FLEX detection kit; All other combinations of antibodies, staining platforms, AR and detection systems yielded staining performance inferior to the clinically validated assay, ranging from variably strong non-specific background to lack of staining. A detailed description with images of the performance of each antibody will be presented at the meeting.

Conclusions: IHC staining for MET equivalent to the clinically validated SP44 IHC assay can be achieved for only 3 of the 9 antibodies using defined staining protocols. Far more rigorous validation studies on clinically annotated tissues are required before an alternative IHC assay to identify MET-positive tumors can be considered.

2165 The Art and Science of Next Generation Sequencing Data Interpretation: Value of Pattern Recognition and Statistical Analysis in Distinguishing True Mutations from Artifacts

S Roy Chowdhuri, MJ Routbort, RR Singh, KA Aldape, R Broaddus, AJ Lazar, BA Barkoh, NG Reddy, LJ Medeiros, R Luthra, KP Patel. University of Texas MD Anderson Cancer Center, Houston, TX.

Background: Next generation sequencing (NGS)-based genotyping is increasingly being implemented in routine clinical testing. Clinical interpretation of NGS data remains a challenge for this relatively new technology with limited user experience and analytic tools. Our laboratory has performed clinical NGS sequencing on more than 4500 solid organ and hematologic malignant tumors. We summarize our experience cataloging mutations and artifacts using two popular NGS platforms.

Design: Multigene mutation profiling was performed using targeted gene panels for mutation hotspots on Ion Torrent PGM (46-gene AmpliSeq panel) and Illumina MiSeq (48 gene TruSeq Cancer panel) platforms. Sequence alignment and variant calling was performed by vendor-provided software solutions. Variant calls were verified by visual inspection of sequenced data in Integrative Genomics Viewer (IGV) from Broad Institute (Cambridge, MA). Suspected artifacts were confirmed or excluded by Sanger or pyro-sequencing. Statistical analysis tools were custom designed to assist with evaluation of sequencing data. An artifact was defined as a variant call that could not be confirmed by a secondary method with comparable sensitivity.

Results: Sequencing patterns for true point mutations, insertions (ins) and deletions (del) tend to be unique, allowing prediction of true versus false-positive calls. Single-base pair ins or dels were the most common types of artifact. The location of a mutation at the end of a sequencing read was the most common factor contributing to a false-negative result, whereas, a homopolymer region was the most common cause of a false-positive call. Ins or dels miscalled as point mutation were also seen. We propose the following categories for attribution of NGS artifacts: type A, platform; type B, analysis run; type C, amplicon; type D, reference sequence; type E, native sequence; and, type F, software or type G, non-specific.

Conclusions: A combination of pattern recognition and ongoing statistical analysis is critical for interpreting next generation sequencing data. Our study provides a catalogue schema for uniform and systematic capture of artifacts on two popular NGS platforms along with the summary of common artifacts for the clinical community.

2166 Multi-Gene Mutational Profiling of Breast Carcinoma Using Next Generation Sequencing (NGS)

S Roy Chowdhuri, M Routbort, KP Patel, R Singh, R Broaddus, A Lazar, A Sahin, G Mills, J Mendelsohn, F Meric-Bernstam, K Aldape, R Luthra. University of Texas MD Anderson Cancer Center, Houston, TX.

Background: Somatic mutations in breast cancer can define prognosis and predict response to therapy. The advent of next generation sequencing (NGS) platforms in the realm of clinical molecular diagnostics has made multi-gene mutational profiling a highly successful methodology for massively parallel sequencing using small quantities of DNA.

Design: Tumor specimens from 405 breast carcinoma patients, including ductal carcinoma, lobular carcinoma, metaplastic carcinoma and carcinoma not otherwise specified were included in the analysis. Tumor samples included formalin-fixed paraffin-embedded (FFPE) core needle biopsies, resection specimens, and cytopathology (cell blocks and direct smears). Ten ng of DNA from each sample was tested for mutations in hotspot regions of 46 cancer related genes (Ion AmpliSeq Cancer Panel) using a 316 or a 318 chip on an Ion Torrent Personal Genome Machine (PGM) Sequencer (Life Technologies, CA).

Results: Mutations were detected in 216/357 (61.5%) patients tested. *TP53* was most frequently mutated (n=109; 30.5%), followed by *PIK3CA* (n=87; 24.4%), *AKT1* (n=17; 4.8%), *ATM* (n=11; 3.1%), *STK11* (n=6; 1.7%), *APC* (n=6; 1.7%), *MET* (n=4; 1.1%), *ABL1* (n=4; 1.1%), and *KRAS* (n=4; 1.1%). *TP53* mutations were often seen in conjunction with *PIK3CA* mutations (n=16). Mutations were detected at a lower frequency (<1%) in *SMAD4, PTEN, EGFR, MLH1, RET, HRAS, MPL, BRAF, ERBB2, FGFR2, SRC, KDR, FGFR1, JAK3, NOTCH1, NRAS* and *ERBB4*. Forty-seven patients were tested for both the primary as well as metastatic tumors, out of which 36 patients (76.6%) showed identical results. Of the 11 patients with discordant results, 10 patients had additional mutations in the metastasis that were not present in the primary tumor, including mutations in *TP53* (n=3), *PIK3CA* (n=2), *APC* (n=1), *KRAS* (n=1), *PTEN* (n=1), *BRAF* (n=1), and concurrent *AKT* and *BRAF* (n=1) mutations.

Conclusions: Our results show that mutations in *TP53* and *PIK3CA* are seen at a higher frequency (30.5% and 24.4%) in breast cancer patients, with other mutations detected infrequently (<5%). Mutational analyses between primary and metastatic tumors were largely concordant with approximately 21% of patients showing additional new mutations in the metastases. In summary, our results show that NGS-based 46-gene mutational profiling using small amounts of DNA can provide useful information regarding mutation status of genes that play a predictive and prognostic role in directing personalized cancer therapy for breast carcinoma patients.

2167 Comparison of Methods for Combined Immunofluorescence with Fluorescence In Situ Hybridization and Visual Optimization by Multispectral Imaging

ET Sadimin, K Walton, L Franciosa, L Cong, X Qi, DJ Medina, RK Strair, H Aviv, LA Goodell, DJ Foran. Rutgers Robert Wood Johnson Medical School, New Brunswick, NJ; Rutgers Cancer Institute of New Jersey, New Brunswick, NJ.

Background: The combination of Immunofluorescence (IF) and Fluorescence In Situ Hybridization (FISH) is a valuable tool in evaluating chromosomal aberrations of specific cell lineages. This method of combining IF and FISH has been referred to in the literature as FICTION (fluorescence-immunophenotyping and interphase cytogenetics as a tool for investigation of neoplasms). Although this technique is very informative, it is technically challenging, thus limiting its use as a routine diagnostic tool. In this study we attempted to optimize the technique by comparing the results of performing FISH before IF (FISH-IF) to IF before FISH (IF-FISH) on frozen tissues, using different fixatives, buffers and incubation procedures. Additionally, we explored the option of utilizing multispectral imaging to enhance visualization when multiple antibodies were used.

Design: Fresh tonsil, kidney and liver tissues were snapped frozen, then cut at 3-4 microns. The (*CCND1/IgH*) and (*IgH/BLC2*) probes were used for the FISH analysis. For IF, we used antibodies for CD5, CD20, FDC, CK7 and CK8/18 coupled with AlexaFluor® 488, 555, 594 or 647. Images are obtained with a multispectral camera attached to a Nikon90i microscope.

Results: The FISH-IF techniques were more consistent and more reproducible compared to the IF-FISH techniques. When IF was performed before FISH, the harsh treatment required to run FISH affected the IF signal, especially in cases using antibodies against weakly expressed antigens. Using the multispectral imaging system significantly improved the image quality by providing sharp, clear visualization of the fluorescence signals, while allowing the use of IF labeling with higher wavelength conjugates (i.e. approaching infrared) which were not readily visible to human eyes. Furthermore, in cases exhibiting multiple colors which are inherently difficult to discern with the naked eye, the digital, multi-spectral system made it possible to enhance the differences through the use of pseudo-colors.

Conclusions: In this study, we have optimized an extremely useful technique that may be utilized clinically for prognostic and treatment purposes. While we have shown that both FISH-IF and IF-FISH give interpretable results, FISH-IF was generally preferred due to its consistency, reproducibility and compatibility with weaker antibodies. Future work will include optimizing the procedures and conditions for paraffin embedded tissues.

2168 Squamous Cell Carcinomas Frequently Stain Positively for the "Adenocarcinoma-Marker" MOC-31: A Diagnostic Pitfall

EC Savage, MP Gailey, AM Bellizzi. University of Iowa, Iowa City, IA.

Background: Immunohistochemistry (IHC) for MOC-31, a monoclonal antibody to epithelial cell adhesion molecule, is frequently used in the "adenocarcinoma (AdCA) vs. mesothelioma (Meso)" and "AdCA vs. hepatocellular carcinoma (HCC)" differential diagnoses, in which it positively stains AdCAs. We have seen pathologists use MOC-31 outside of these select contexts as an "AdCA marker" [e.g., to support a diagnosis of AdCA over squamous cell carcinoma (SCC)]. MOC-31 was actually initially raised against a small cell carcinoma cell line, and although poorly documented, we have encountered MOC-31-positive SCCs, which in several instances were initially misclassified as AdCAs based on this result. The purpose of this study is to document MOC-31-positivity in SCCs.

Design: MOC-31 IHC was performed on whole sections of 110 SCCs from diverse anatomic sites. For comparison, we also tested expected negative (10 Mesos, 10 HCCs) and positive [5 neuroendocrine carcinomas (NECs), 6 lung AdCAs metastatic to pleura, 6 colon AdCAs metastatic to liver] tumor types. Finally, we tested tumor types of uncertain reactivity [11 urothelial carcinomas (UCs), 5 midgut neuroendocrine tumors (NETs), 5 pancreatic NETs]. Cases were scored for extent (%) and intensity (0, 1+, 2+, 3+) of membranous staining and an H-score calculated (extent x intensity). For the SCCs, grade (well, moderately, poorly differentiated) was extracted from the pathology report.

Results: Frequency of MOC-31-positivity and mean H-scores for SCCs by anatomic site and for all tumor types are given in Tables 1 and 2.

Table 1: MOC-31-Positivity in SCCs by Anatomic Site

	% Positive	Mean H-score (if Positive)
Anus (n=10)	40	86
Cervix (n=12)	83	66
Esophagus (n=7)	71	74
Larynx (n=10)	30	36
Lung (n=14)	79	95
Penis (n=11)	9	20
Skin (n=11)	0	NA
Tongue (n=14)	50	67
Vagina (n=10)	40	110
Vulva (n=11)	0	NA

Table 2: MOC-31 Positivity by Tumor Type

	% Positive	Mean H-score (if Positive)
SCC	41	77
Meso	0	NA
HCC	20*	68
NEC	60	63
Lung AdCA	100	158
Colon AdCA	100	281
UC	55	69
Midgut NET	100	273
Pancreatic NET	80	130

* these expressed HepPar1 and glypican-3

50% (18/36) of poorly differentiated, 41% (23/56) of moderately differentiated, and 13% (2/16) of well-differentiated SCCs were MOC-31-positive.
Conclusions: SCCs are frequently MOC-31-positive (~40%), especially in lung and esophagus, where distinction of SCC from AdCA is therapeutically critical, and in poorly differentiated tumors, in which distinction is the most difficult. UCs are also often positive, while NETs are intensely positive, similar to AdCAs. Pathologists are cautioned against relying on MOC-31 IHC to diagnose AdCA.

2169 Importance of Tumor Banking Infrastructure in Personalized Medicine: An Approach from a Head and Neck SPORE Neoplasm Database

H Singh, W Amin, AM Egloff, JE Bauman, L Wang, JL Hetrick, JR Grandis, AV Parwani. University of Pittsburgh, Pittsburgh, PA; University of Pittsburgh Medical Center, Pittsburgh, PA.
Background: The Personalized Medicine is the new frame work for the study of disease through new measurements, visualization and computational technologies to replace current, largely reactive mode of medicine with approaches for assessing the individual risks on the basis of presence and absence of certain variables. The Specialized Program of Research Excellence (SPORE) Head and Neck Tumor Database is a bioinformatics supported system that hosts large and qualitative data from patients with head and neck malignancies. Over the last seven years, the database has provided de-identified information to researchers to facilitate the discovery of novel biomarkers, new therapeutic approaches, and pave the way for the delivery of evidence based health care to patients.
Design: The database provides a web-based data annotation and query engine based on common data elements (CDEs). The system is supported in a three-tiered architecture implemented on an Oracle AS v10.1.2.3 and Oracle RDBMS v.11.1.0 on a Community Enterprise Operating Systems (**Centos 5.3**) virtual host definitions which is supported by IBM Cluster hardware. The database is built to provide semantic and syntactic interoperability.
Results: The database currently holds 8862 cases and provides demographic, clinical, pathology, treatment, follow-up, patient and tumor genomic sequencing and other molecular data for 14234 tumor accessions. Recent integration and links to whole genome sequence data has boosted the usability of the database for studying trends and carrying out predictive analyses. This database allows access to sequence analysis data results and is flexible enough to accommodate additional data set needs as they arise.
Conclusions: The database provides informatics support to facilitate basic, clinical and translational science research to support personalized medicine efforts in head and neck cancer. It offers a mechanism to efficiently select and access richly-annotated bio specimens to meet the research interests and requirements with the goal of integrating laboratory data from multiple investigators in order to develop comprehensive characterization of traits and treatment outcomes. The tool protects patient privacy by providing only de-identified data with Institutional Review Board and SPORE Scientific Committee Review and approval.

2170 Quantitation and Detection of *BRAF* V600E Mutation by Allelic Discrimination Real-Time PCR

D Sirohi, Y Wang, LR Jonathan, V Kumari, D Xu, MX Wang, WB Furmaga, H Fan. University of Health Science Center at San Antonio, San Antonio, TX; Providence Sacred Heart Medical Center & Children's Hospital, Spokane, WA; University of Missouri School of Medicine, Columbia, MO.
Background: The *BRAF* V600E mutation has been identified in various tumors, mainly in melanoma, papillary thyroid carcinoma (PTC), hairy cell leukemia (HCL), and colorectal cancer (CRC). Quantitation and detection of the V600E are not only useful for molecular targeting therapy, but also for monitoring minimal residual disease. We validated a laboratory developed test - quantitative allelic discrimination real-time PCR (Q-AD-PCR) assay that can both detect the V600E mutation and quantitate the mutation load.
Design: DNA was extracted from 74 clinical samples (9 melanoma, 8 PTC, 2 HCL, 23 CRC, 6 benign thyroid tissue, 15 non-HCL hematologic disorder, and 11 exchange samples), which included 46 formalin fixed paraffin embedded tissue (FFPE) and 28 blood, bone marrow, or frozen tissue. The samples were simultaneously analyzed for the presence and mutation load of V600E by Q-AD-PCR assay. The assay utilizes a set of primers combined with two TaqMan MGB probes labeled with VIC or 6-FAM, targeting wild-type (T) or mutant (A) allele respectively, to detect the V600E mutation. The relative quantitation of V600E is determined by comparing results to a V600E homozygous melanoma cell line (ATCC HTB-72D). Assay conditions were optimized, and the assay's accuracy, specificity, sensitivity, linearity and reproducibility were assessed.
Results: Assay accuracy was tested by comparing Q-AD-PCR results from 50 specimens that had been analyzed by other methods (27 by Sanger sequencing, and 23 by INFINITI Analyzer). Result agreements were obtained on 48/50 samples. Although the Q-AD-PCR is designed to detect the V600E mutation, 2 cases with V600K and V600E2 were also detected by the assay due to cross reactivity. No mutation was detected on 21 normal or non-HCL cases, confirming the assay's specificity. The assay was linear between 6-100% and sensitive to 6% mutant. The reproducibility was evaluated by analyzing 35 replicates (2-fold serial dilutions of HTB-72D representing 100% to 6% mutant) on different days, with average inter-assay coefficients of variation of 7-24%. V600E was detected in 16/74 (22%) clinical samples with mutation loads ranging from 11-86% and a median of 63%.
Conclusions: The Q-AD-PCR assay is a rapid, reliable, and sensitive method for simultaneously obtaining quantitative and qualitative *BRAF* V600E mutation results on routine clinical samples, especially FFPE specimen.

2171 Comparison of Molecular Oncology Tests in Cytology Smears and Formalin-Fixed, Paraffin-Embedded Tissue

AN Snow, MP Gailey, AA Stence, JA Pruessner, D Ma. University of Iowa, Iowa City, IA.
Background: Fine needle aspiration (FNA) is widely used clinically due to its tolerance by the patients and relative non-invasive nature. Formalin-fixed paraffin-embedded (FFPE) cell blocks are routinely used for molecular oncology testing in the clinical laboratory. A pitfall of cell block is the inability to assess cellularity before preparation, which can result in insufficient tumor cells for molecular testing. In this case, additional surgical procedures may be needed to procure adequate tissue for testing. We validated a method of DNA extraction directly from cytology smears and compared the results of multiple molecular oncology tests using DNA extracted from cytology smears and FFPE tissue from the same patients.
Design: Thirteen FNA cases were selected from archived cases that had molecular tests performed previously on FFPE tissue at our molecular pathology laboratory. Areas with tumor were marked by a cytopathologist. A matrix capture solution (Pinpoint Slide DNA Isolation, Zymo Research, CA) was applied. Tissue bound to the solution was microdissected and genomic DNA was isolated according to the manufacturer's instructions. Both Diff-Quik (DQ) and Papanicolaou (PAP) slides were included.
Results: The minimal DNA yield was 60 ng per 100 tumor cells. The quality of DNA was evaluated by optical densitometry (ratio of OD 260 nm/280 nm). Mutations detected included *BRAF* V600E in anaplastic and papillary thyroid carcinomas by Sanger sequencing and primer extension assays, an 18 base pair deletion and point mutations in the *EGFR* gene of lung adenocarcinomas using Sanger sequencing, and a G12S mutation in the *KRAS* gene from a metastatic colon cancer by primer extension. As a proof of concept, a multiplex PCR-based assay for microsatellite instability (MSI) from an MSI-high colon cancer was also performed. There was 100% concordance between DNA obtained from cytology smears and FFPE tissue. The DNA also performed well on the Ion AmpliSeq™ Cancer Hotspot Panel v2 (Life Technologies, Carlsbad, CA). The sensitivity and specificity of the tests were not compromised when the input DNA extracted from the smears was decreased 10-fold.
Conclusions: The cytology smear is a reliable source for molecular oncology testing. We observed 100% concordance between DNA isolated from cytology smears and FFPE tissue, which included a variety of tumors, mutations and test platforms. Both DQ and PAP stained slides are equally suitable for testing. The use of cytology smears for molecular oncology testing is cost-effective and can save patients from additional/more invasive procedures to obtain tissue for testing.

2172 Myc IHC Predicts *MYC* Rearrangements by FISH

KA Stevens, C Cohen. Emory University School of Medicine, Atlanta, GA.
Background: *MYC* is the proto-oncogene classically associated with Burkitt lymphoma (BL) located at chromosomal locus 8q24. Rearrangements of *MYC* are seen in nearly 100% of BL, but are reported in 3-16% of Diffuse Large B-cell Lymphomas (DLBCL). Rearrangements of *MYC* are usually tested for by fluorescent in-situ hybridization (FISH); however, a monoclonal antibody directed against the human Myc protein for use in immunohistochemistry (IHC) is now available (Epitomics, clone Y69). We compared IHC to the current FISH method.
Design: 31 cases were identified that had been tested for MYC rearrangements by FISH over 27 months with heterogeneity in the diagnoses: 5 BL; 10 DLBCL; 3 B-cell lymphoma unclassifiable between DLBCL and BL; 5 B-cell lymphoma not otherwise specified; 1 EBV-related B-cell lymphoma; 1 composite CLL/SLL-large cell lymphoma, and 6 designated as high-grade or aggressive B-cell lymphoma. Analysis by FISH was performed as part of the clinical work-up, where a MYC rearrangement is defined as a split fusion signal in at least 5.7% of cells. Myc-IHC was interpreted in each case by the authors, blinded to the FISH result, as a qualitative positive (overexpressed) or negative (not overexpressed) result. Cases considered positive showed strong Myc nuclear staining in nearly 100% of the tumor cells, whereas cases considered negative were either completely negative or showed staining in a smaller percentage of cells.
Results: 12 cases (39%) were positive for MYC rearrangements by FISH, including all 5 cases of BL and 7 additional cases: 3 high-grade B-cell lymphoma, 2 B-cell lymphoma unclassifiable between DLBCL and BL, 1 DLBCL, and 1 B-cell lymphoma NOS. Overall, 13 cases (42%) showed Myc overexpression by IHC, 11 (85%) of which harbored a MYC rearrangement by FISH. One case of DLBCL that showed a MYC rearrangement by FISH was negative by IHC (false negative). One case of B-cell lymphoma unclassifiable between DLBCL and BL and one case of B-cell lymphoma NOS showed Myc-overexpression by IHC, but did not show a rearrangement by FISH (false positives). Thus, Myc-IHC predicted a MYC-rearrangement by FISH with 92% sensitivity and 89% specificity. The positive predictive value in this group of morphologically aggressive lymphomas was 85% and the negative predictive value was 94%.
Conclusions: Myc-IHC predicts *MYC* rearrangements by FISH with high sensitivity and specificity. There was one false negative and two false positives. Myc-IHC is a potentially useful screening tool for identifying lymphomas that may harbor a MYC-rearrangement. It is easier and quicker to perform than FISH, thus offering potential cost and time savings.

2173 Implementation of a Next Generation Sequencing Assay for Tumor Profiling in a Clinical Laboratory

JA Thorson, S Sun, D Brown, B Datnow, S Murray. UC San Diego, La Jolla, CA.
Background: Increasing demands are placed upon clinical laboratories to provide timely, clinically actionable, and analytically valid information regarding the genomic profile of tumor specimens. Next-generation sequencing (NGS) technologies offer one means of meeting this need. Transitioning this technology into routine clinical practice requires not only analytical validation but also more significantly the creation

of an integrated process encompassing all steps from order entry to result reporting.
Design: We have performed analytical validation of an NGS-based test comprised of key exons in 47 clinically relevant genes for solid tumors. Validation specimens included 52 FFPE tumor specimens from various organ types with previously known mutational status. Infrastructure to enable specimen and dataflow was created, beginning with direct order entry in the hospital information system (HIS), triggering requests for tissue block retrieval and collection of a paired peripheral blood sample. Amplicon-based Illumina sequencing libraries are created using DNA from each specimen and sequenced to a minimum coverage of 500X on a MiSeq instrument (Illumina). A custom bioinformatics analysis pipeline is employed, using vendor-supplied software as well as in-house designed scripts for quality metric analysis and annotation. Reportable variants are confirmed by Sanger analysis. A final report, using HGVS naming conventions for variants, characterizing each as somatic versus germline, and providing a narrative interpretation of the clinical significance is transferred to the HIS and is available in discrete element display as well as in a formatted, PDF version via hyperlink.
Results: Reproducibility using progressively diluted samples was excellent for single nucleotide variants and small indels at 10% variant frequency. Of 52 FFPE specimens, 31/52 (60%) yielded analyzable DNA. All variants identified by NGS were confirmed via Sanger analysis with 100% concordance. In addition, results for variants within the genes included in the panel were highly concordant with those obtained by an outside reference laboratory. At a throughput of 12 samples/week (6 paired tumor/blood samples or 12 tumor samples), turn-around time from order to result availability is 14 to 16 days.
Conclusions: Our findings show that NGS technology can be successfully integrated into a clinical laboratory environment and provide improvements in service necessary to meet the demands of personalized therapeutics. Challenges remain with the use of FFPE tissue for analysis. Studies evaluating fixation conditions may provide improvement in this regard.

2174 Correlation of Image Analysis-Assisted Detection of Monoclonal Plasma Cells in Bone Marrow Tissue Sections Using In-Situ Hybridization (ISH) Versus Serum Free Kappa and Lambda Light Chain Ratio and Immunofixation Electrophoresis (IFE) Studies in Patients with Plasma Cell Myeloma (PCM) Following Bone Marrow Transplantation

RK Walsh Jahnke, L Tilzer, J Woodroof. Kansas University Medical Center, Kansas City, KS.
Background: Detection of monoclonal paraproteins using serum IFE and serum free light chain ratio (FLC) plays a pivotal role in screening, diagnosis and follow up of patients with PCM. Quantitation and demonstration of monoclonal plasma cell populations by ISH for kappa and lambda on bone marrow (BM) tissue sections also contributes to monitoring patients with PCM. Correlation of serum IFE and FCL ratio with results of bone marrow evaluation is presented.
Design: We identified 182 specimens from 110 patients with myeloma submitted between 2012 and 2013. ISH studies for kappa and lambda light chains obtained on formalin-fixed BM tissue sections were analyzed using a novel algorithm built using Aperio® Scanscope software.

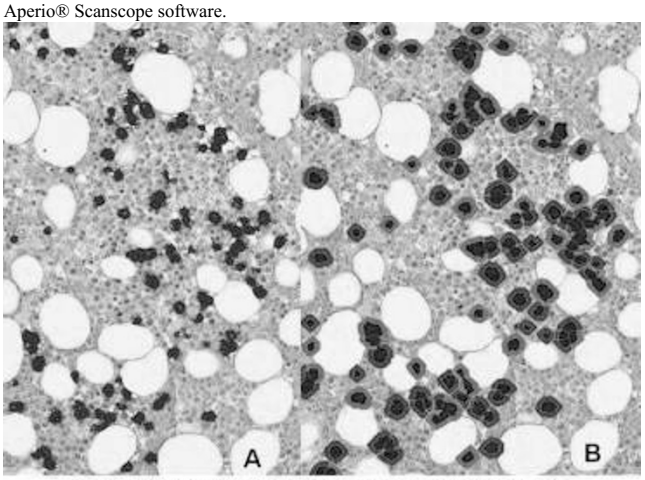

Figure 1: A) ISH Kappa stain B) Resultant Aperio® Imagescope analysis of same slide

Image analysis data included ISH K/λ ratios and absolute PC count per millimeter squared. These results were compared with serum FLC K/λ ratio, and serum IFE results. Each test result was categorized as positive or negative for monoclonal paraprotein, and correlation of results from the three techniques was done.
Results: Results from all three techniques correlate in only 45% (n=81) of specimens. IFE was positive in approximately 30% of cases with negative ISH and FLC, whereas, ISH and FLC were positive in 10% of cases with a negative IFE result. ISH and FLC results correlated with each other in 70% of cases. Cases with no correlation between ISH and FLC had a significantly smaller plasma cell concentration than cases that did correlate ($p<0.05$).
Conclusions: Our findings demonstrate that these 3 methods do not show a high level of correlation. IFE was the most sensitive in detection of monoclonal paraproteins, with ISH and FLC both showing negative results in 30% of cases with a positive IFE. This study suggests that FLC ratio may have limitations in the detection of low levels of monoclonal paraproteins. This study also introduces a novel use of image analysis for the quantitation and measurement of the kappa/lambda ratio of plasma cells in tissue slides evaluated with in situ hybridization.

2175 Utilization of Tumor Cell Enriched Cell Transfer Technique in Detection of EGFR and KRAS Mutation on Small Biopsies of Patients with Diagnoses of Adenocarcinoma

HH Wu, M Randolph, KM Post, JD Sen, AJ Malek, L Cheng. Indiana University School of Medicine, Indianapolis, IN.
Background: Performing molecular testing to identify EGFR and KRAS mutations on newly diagnosed advanced staged non-small cell lung cancers in a timely fashion has become the standard of care. False negative results may occur when there are scant tumor cells on the sections. A novel tumor cell enriched cell transfer technique (CTT) was evaluated for its utilization for the molecular testing.
Design: A computerized search of the laboratory information system was performed. Cases with diagnoses of adenocarcinoma and had previously EGFR and/or KRAS performed on the formalin-fixed paraffin embedded (FFPE) biopsies were identified. The archived H&E stained slides that were previously cut for the molecular testing were reviewed and the tumor cells were selected with marking. The marked tumor cells were removed through CTT and submitted for EGFR (8 cases) and KRAS mutations (7 cases). The results were correlated to the previous reports of which the molecular testing was performed on the recut of the FFPE.
Results: The PCR-based molecular testing was successfully performed on 13 of 15 CTT samples (8/8 cases for EGFR and 5/7 cases for KRAS mutations). 11 of 13 CTT samples show correlation with previous results including 1 mutation and 5 wild types for EGFR and 1 mutation and 4 wild types for KRAS. Two EGFR mutations (both L858R) were identified on the CTT samples but were reported as negative on FFPE. Multiple immunohistochemical stains were performed on theses two false negative cases before the molecular testing was ordered and the recut of the H&E-stained sections revealing tumor cells present focally in some but not all the cores that were submitted.
Conclusions: The ability to visualize and select higher concentration of tumor cells through the CTT provides an advantage over the recut of the FFPE block, especially when the tumor cells are fewer and the surrounding normal tissues are abundant in the block. CTT is a feasible alternative method for cases that containing scant tumor cells on the biopsies to perform molecular testing.

2176 Pancreas Cystic Lesions: Molecular Abnormalities and Its Relationship of FNA Cyst Fluid Cellularity and Clinical Findings

J Xie, B Corcoran, S Finkelstein, JF Silverman. Allegheny General Hospital, Pittsburgh, PA; RedPath Integrated Pathology, Inc, Pittsburgh, PA.
Background: Cytologic evaluation of pancreatic cysts (PC) can be diagnostically challenging especially when either low epithelial cellularity or acellular specimens are encountered in the FNA cytology specimen. We evaluated the role of molecular analysis as an aid for a more specific diagnosis in FNA of PC having no epithelial cells.
Design: A large, consecutive series of 608 cases of PC FNA were retrospectively evaluated. EUS findings accessed as potentially aggressive included PC size $\geq$ 3 cm, duct dilation $\geq$ 1 cm, solid component formation and CEA level over 1000 ng/ml. Molecular analysis targeted three abnormalities associated with aggressive disease: 1) high concentration of DNA, 2) oncogene point mutations of KRAS/GNAS and 3) the presence of multiple tumor suppressor genes loss assessed by loss of heterozygosity (LOH) using a panel of 24 microsatellite markers. PC was classified as high risk by correlated the molecular results with cytologic cellularity and clinical findings.
Results: 456 of the 608 PCs (75%) cases were found to lack epithelial cells. This large PC subset lacking diagnostic epithelial cells (PC-epith) was compared to the remaining PC containing epithelial cells (PC+epith). We found that there is evidence of biologic aggressiveness present in both subsets, but the incidence of CEA level over 1000 ng/ml, KRAS mutation, multiple LOH mutations and high risk status in the PC+epith groups are statistically higher than in the PC-epith group ($P< 0.05$).

Table 1

	PC-epith %	PC+epith %
Cyst size ≥ 3cm	19	21
Duct dilation ≥ 1 cm	3	2
Solid component formation	11	12
CEA level 192-1000 ng/ml	22	18
CEA level >1000 ng/ml*	21	30
High DNA concentration	17	24
KRAS mutation*	21	32
GNAS mutation	3	5
Multiple LOH mutations*	4	10
'High Risk' by integrated clin/mol*	11	18

The numbers of PC-epith and PC+epith cases are 456 and 152, respectively. *p<0.05, Chi Square test

Conclusions: 1) The presence of epithelial cells in FNA of pancreas cysts have a higher risk of malignancy compared to aspirates without epithelial cells. 2) However, molecular analysis is able to define a subset of cases lacking epithelial cells as "high risk" for potential aggressive disease.

2177 Automated Branching DNA RNA In Situ Hybridization for the Detection of Multiple Transcripts

MB Yaylaoglu, S Sa, H Koeppen. Genentech, South San Francisco, CA.
Background: Existing non-isotopic RISH methods frequently utilize multiple enzymatic amplification steps which can lead to non-specific signal. Furthermore when trying to co-detect transcripts it is very difficult to prevent cross-reaction of the chemistry used to detect the separate RNA targets. We have utilized RNA-specific oligonucleotide probes with branched DNA signal amplification for an assay that allows us to detect four distinct transcripts in a single tissue section.
Design: This protocol uses gene-specific type 1 probe sets (Affymetrix QuantiGene ViewRNA) on a robotic platform to detect multiple transcripts by non-radioactive ISH with branching DNA amplification to specifically increase sensitivity. Instead of

simultaneous hybridization of multiple probes our method employs successive probe hybridization, amplification, and development of substrate signal for each RNA target molecule, followed by removal of probe and associated DNA branches by a high-stringency wash. Steps are illustrated in figure 1. A single-plex, and a standard dapB negative control was run in parallel for each probe.

Figure 1. Outline of protocol for detection of multiple gene transcripts. Steps in bracket were repeated 3 times to successively detect 4 gene transcripts.

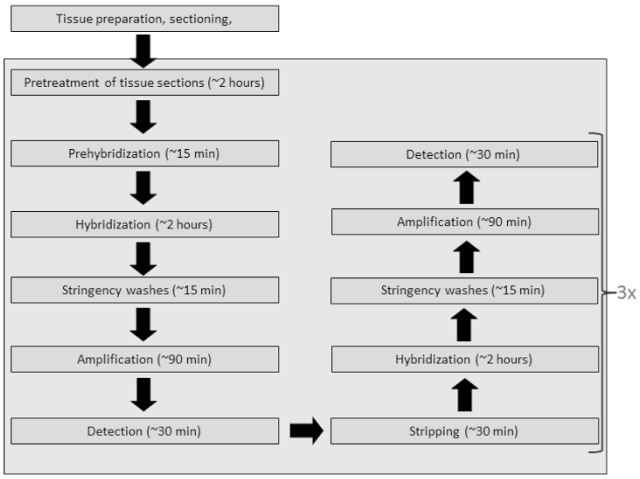

Results: Data are presented for co-expression of interneuron markers in adult mouse brain in figure 2. Formalin-fixed, paraffin-embedded coronal sections from adult mouse brain were used for successive hybridization with four different gene-specific probe sets for 4 interneuron markers: Somatostatin (Sst), Parvalbumin (Pvalb), Vasoactive intestinal polypeptide (Vip), Neuropeptide Y (Npy).

Figure 2. Four interneuron markers: Somatostatin (Sst), Parvalbumin (Pvalb), Vasoactive intestinal polypeptide (Vip), Neuropeptide Y (Npy).

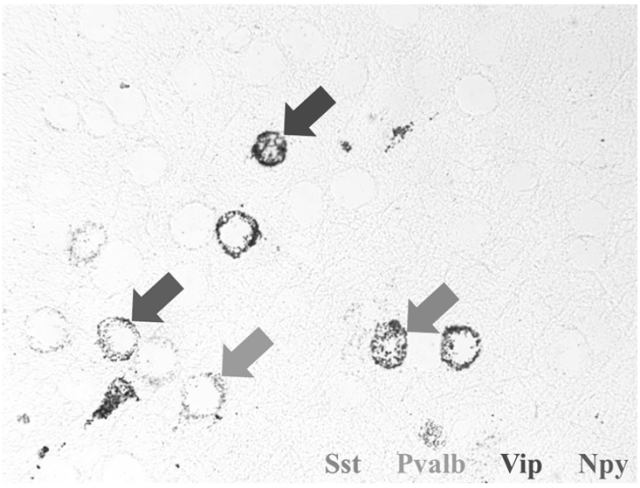

Conclusions: Sequential ISH using gene-specific oligonucleotide probes with branched DNA signal amplification allows for sensitive and specific detection of multiple distinct RNA target transcripts in the same tissue section without a decrease in the sensitivity and specificity of the assay. This method is valuable not only for the co-localization of marker expression but also in circumstances when tissue resources are limited.

2178 A Novel Computerized Image Analysis Method to Differentiate Malignant Mesothelioma from Reactive Mesothelial Proliferations in Effusion Cytology Specimens

O Yergiyev, AB Tosun, GK Rohde, JF Silverman. Allegheny General Hospital, Pittsburgh, PA; Carnegie Mellon University, Pittsburgh, PA; West Penn Hospital, Pittsburgh, PA.

Background: Differentiating malignant mesothelioma (MM) from reactive mesothelial proliferations (RMP) is based on demonstrating tissue invasion. While pleural effusion specimens can yield cells for cytologic examination, it is insufficient to make the definitive diagnosis of MM since tissue invasion cannot be assessed. We evaluated a novel image analysis technique which can potentially differentiate MM from RMP based on the patterns of chromatin distribution in the nuclei of mesothelial cells in effusion cytology specimens.

Design: 34 cases were selected from the pathology database of two tertiary care academic centers, including 16 cases of MM and 18 cases of RMP. All patients had both a pleural effusion cytology specimen and pleural biopsy with histologic confirmation. Diff-Quik stained slides from each case were reviewed, and digital images of mesothelial cells were acquired using standard imaging equipment. 1080 individual nuclei were segmented using original software. After drawing the nuclear contours, the luminance component of segmented nuclei was analyzed. The images were first normalized to remove relative translations and rotations. After normalization, the chromatin content of each segmented nucleus was processed to obtain its linear optimal transport (LOT) embedding. A linear classification function was computed for each individual nucleus to distinguish it from the two classes (benign and malignant) by using the modified Fisher Linear Discriminant Analysis (PLDA) technique on the LOT embedding. A set of nuclei from each patient was then classified using a majority voting strategy.

Results: We utilized the standard "leave one patient out" cross validation strategy to classify the cases. Each patient was diagnosed by using the above classifier, computed without using nuclei from that patient. In each classification task the same number of nuclei for each class was used. With the above technique, we were able to classify the effusion cytology cases as benign or malignant with 100% accuracy when compared to the histologic diagnosis.

	Predicted	
Actual	**Benign**	**Malignant**
Benign	18	0
Malignant	0	16
Accuracy	100%	

Table 1. Study results.

Conclusions: We present an original computerized technique with a potential to differentiate between MM and RMP based on the nuclear structure of mesothelial cells in effusion cytology specimens, that may alleviate the need for an invasive procedure.

Ultrastructural Pathology

2179 Three Year Follow Up in an Allograft Kidney from a Metachromatic Leukodystrophy Donor – Ultrastructural Findings

S Ballal, N Sondheimer, S Koutzaki, A Doyle, S Soundararajan. Drexel University College of Medicine, Philadelphia, PA; The Children's Hospital of Philadelphia, Philadelphia, PA.

Background: Metachromatic leukodystrophy(MLD) is an inherited disorder of myelin metabolism associated with neurodegenerative changes and deposition of metachromatic sulfatide granules in the nervous system. Viscera with excretory functions are also affected. Ultrastructural studies of the kidney in MLD reveal lamellar or zebroid inclusions bound by a single unit membrane. Organs of these patients have rarely been used for donation.

Design: We present the ultrastructural findings over a three year period of a successfully transplanted kidney from a 10 year old MLD donor, diagnosed at age 2 who suffered cardiac arrest. His kidney was transplanted into a 61 year old woman with diabetic nephropathy. Post-transplant course was uncomplicated, with immediate graft function. Currently, the patient is well with creatinine of 1.1mg/dl.

Results: Annual surveillance biopsies revealed acute cellular rejection at 1 year and mild patchy interstitial fibrosis and tubular atrophy at 3 years. Electron microscopic examination revealed intra-cytoplasmic membrane bound concentrically arranged dense laminated inclusions ranging from 1-2μm in the proximal and distal tubules.

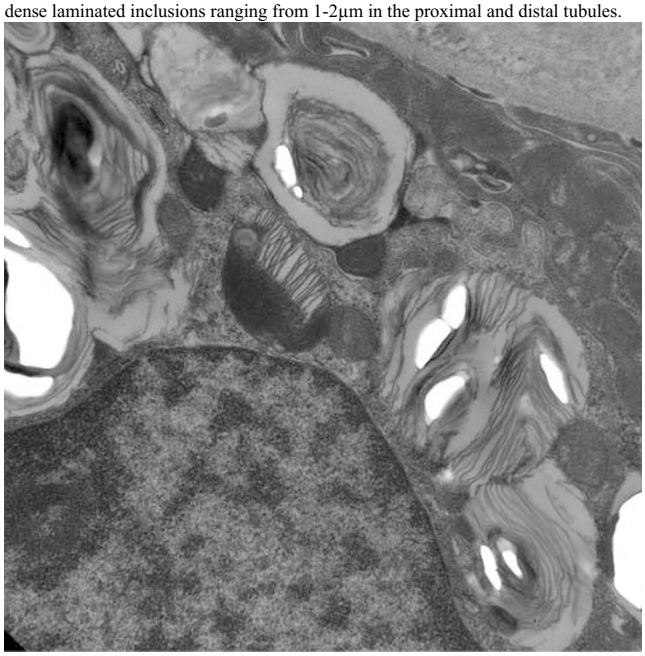

At 3 years, the inclusions are intralysosomal, fragmented and dispersed within the cytoplasm of the affected tubules. There is focal disruption of the brush border through which they are extruded.